Since January 2020 Elsevier has created a COVID-19 resource centre with free information in English and Mandarin on the novel coronavirus COVID-19. The COVID-19 resource centre is hosted on Elsevier Connect, the company's public news and information website.

Journal of Infection 80 (2020) 469–496

Contents lists available at ScienceDirect

Journal of Infection

journal homepage: www.elsevier.com/locate/jinf

Letters to the Editor

Analysis of angiotensin-converting enzyme 2 (ACE2) from different species sheds some light on cross-species receptor usage of a novel coronavirus 2019-nCoV

Dear Editor,

A novel coronavirus from Wuhan in central China, named 2019-nCoV, has recently caused an epidemic of pneumonia in humans and posed a huge threat to global public health.[1,2] To the date 06/02/2020, 2019-nCoV has led to more than 31,000 confirmed cases and 637 deaths in China according to National Health Commission of the People's Republic of China (http://en.nhc.gov.cn/index.html). Cases have also been documented in a growing number of other international locations, including the United States (https://www.cdc.gov/coronavirus/2019-ncov/index.html). As a consequence, it is urgent to develop effective measures to control this novel coronavirus on the basis of its pathogenesis.

Host receptor recognition is a determinant for virus infection. During the time of this letter preparation, three works have just been published to explore the receptor usage of 2019-nCoV. A work by Zheng-Li Shi et al. has shown that angiotensin-converting enzyme 2 (ACE2), the receptor for severe acute respiratory syndrome coronavirus (SARS-CoV),[3] from human, *Rhinolophus sinicus* bat, civet, swine but not mouse mediate 2019-nCoV infection *in vitro*, while the detailed mechanisms are not yet determined.[4] The other two works have reported or predicted human ACE2 usage of 2019-nCoV in a similar way to SARS-CoV mainly based on the coronavirus spike (S) glycoproteins.[5,6] Considering the fact that the S proteins mutate and gain capability to recognize host receptors among species,[7,8] there is still a lack of analyses on receptor usage of 2019-nCoV from the receptor perspective, which does not evolve as quickly as viruses.

Here, we firstly performed amino acid sequence alignment of ACE2 from different species, including human, five non-human primates (gibbon, green monkey, macaque, orangutan and chimpanzee), two companion animals (cat and dog), six domestic animals (bovine, sheep, goat, swine, horse and chicken), three wild animals (ferret, civet and Chinese horseshoe bat) and two rodents (mouse and rat). The alignment by Clustal W 2.1 shows that they share a high sequence similarity except chicken (data not shown). The result suggests that 2019-nCoV of probable bat origin may not interact with chicken ACE2 and subsequently infect them, which were not considered in the following analyses. In ACE2, the regions at position 30–41, 82–84 and 353–357 are demonstrated to be involved in the interaction with SARS-CoV S protein, where the residues at positions 31, 35, 38, 82 and 353 are critical.[9] Therefore, we took a close comparison in these regions and residues. As shown in Fig. 1, human and non-human primates share the identity sequences in the regions and residues, implying that ACE2 from non-human primates may recognize 2019-nCoV and mediate its infection. As a result, non-human primates may be susceptible to 2019-nCoV and serve as animal models for antiviral research or intermediate hosts for cross-species transmission. In Fig. 1, the residues of most companion, domestic and wild animals are conserved, especially for the critical ones stated above, while certain ones are variable. For example, Lys31, Glu35, Asp/Glu38 and Lys353 are conserved, which probably form salt bridges. Interestingly, the changes at positions 31, 38 and 82 are observed. These changes suggest steric hindrance and electrostatic interference for host-virus interaction. Taking civet ACE2 as an example, the change of Lys31 to Thr31 is likely to form a hydrogen bond instead of a salt bridge. In addition, the polar side chain of Thr82 may influence the hydrophobic interaction of the original Met82. All these changes may result in a lower binding affinity. However, an additional region covering residues 90–93 has been shown to be involved in civet ACE2 binding to SARS-CoV and enhance their interaction.[10] Consequently, we can't preclude the existence of other regions to compensate for the residue changes. With most residues in human ACE2, the ones from these compaion, domestic and wild animals may be favorable for 2019-nCoV recognition, which is in consistent with the recent work by Zheng-Li Shi et al. In case cross-species transmission, close contact with sick or asymptomatic companion, domestic and wild animals should be cautious, such as for workers in livestock farming and travellers in the wild.

In contrast, certain significant changes occur in the mouse and/or rat ACE2 compared to the human one (Fig. 1). The Asn31 and Ser82 in mouse ACE2 may not form favorable interactions with 2019-nCoV due to their electrostatic or hydrophilic characteristics. Importantly, the change into His353 in both mouse and rat ACE2 does not form a strong salt bridge as Lys353 does. Since the structural information for mouse and rat ACE2 is unavailable, we carried out homology modeling using human ACE2 (PDB code 2AJF) as template on online (https://swissmodel.expasy.org) for further analyses. In Fig. 2A, the change into Ser82 in mouse ACE2 may interfere with the hydrophobic interaction of the original Met82. Additionally, the changes into Asn31 and His353 definitely affect the salt bridge formation and electrostatic potential. The change into His353 in rat ACE2 is similar in the effect on receptor-virus interaction (Fig. 2B). These analyses partially explain why mouse ACE2 does not mediate 2019-nCoV infection reported by Zheng-Li Shi et al. and assume that rodents are not likely to be the susceptible host.

In conclusion, we conducted sequence and structural analyses of angiotensin-converting enzyme 2 (ACE2) from different species, which sheds some light on cross-species receptor usage of 2019-nCoV. All these analyses raise an alert on a potential interspecies transmission of 2019-nCoV and propose further surveillance in other animal populations. Structural studies on human and other species ACE2 in complex with 2019-nCoV spike protein will con-

https://doi.org/10.1016/j.jinf.2020.02.013

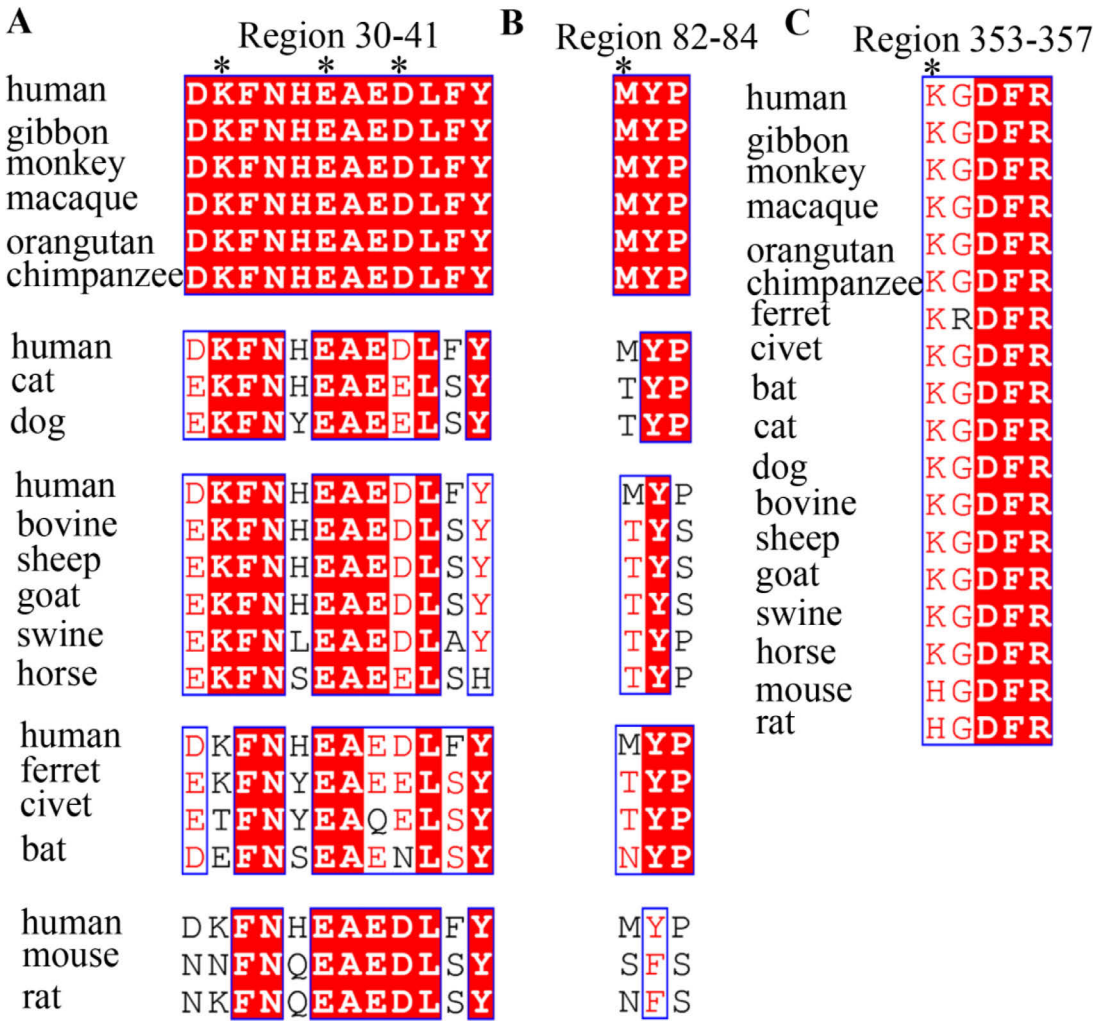

Fig. 1. Sequence alignment of ACE2 from human (UniProt entry Q9BYF1), Northern white-cheeked gibbon (UniProt entry G1RE79), green monkey (UniProt entry A0A0D9RQZ0), crab-eating macaque (UniProt entry A0A2K5X283), Sumatran orangutan (UniProt entry Q5RFN1), chimpanzee (UniProt entry A0A2J8KU96), cat (UniProt entry Q56H28), dog (UniProt entry J9P7Y2), bovine (UniProt entry Q58DD0), sheep (UniProt entry W5PSB6), goat (UniProt entry A0A452EVJ5), swine (UniProt entry K7GLM4), horse (UniProt entry F6V9L3), ferret (UniProt entry Q2WG88), civet (UniProt entry Q56NL1), Chinese horseshoe bat (UniProt entry E2DHI7), mouse (UniProt entry Q8R0I0) and rat (UniProt entry Q5EGZ1). (A) Region 30–41. (B) Region 82–84. (C) Region 353–357. The conserved residues in the regions are colored in red and the critical residues are marked by asterisks.

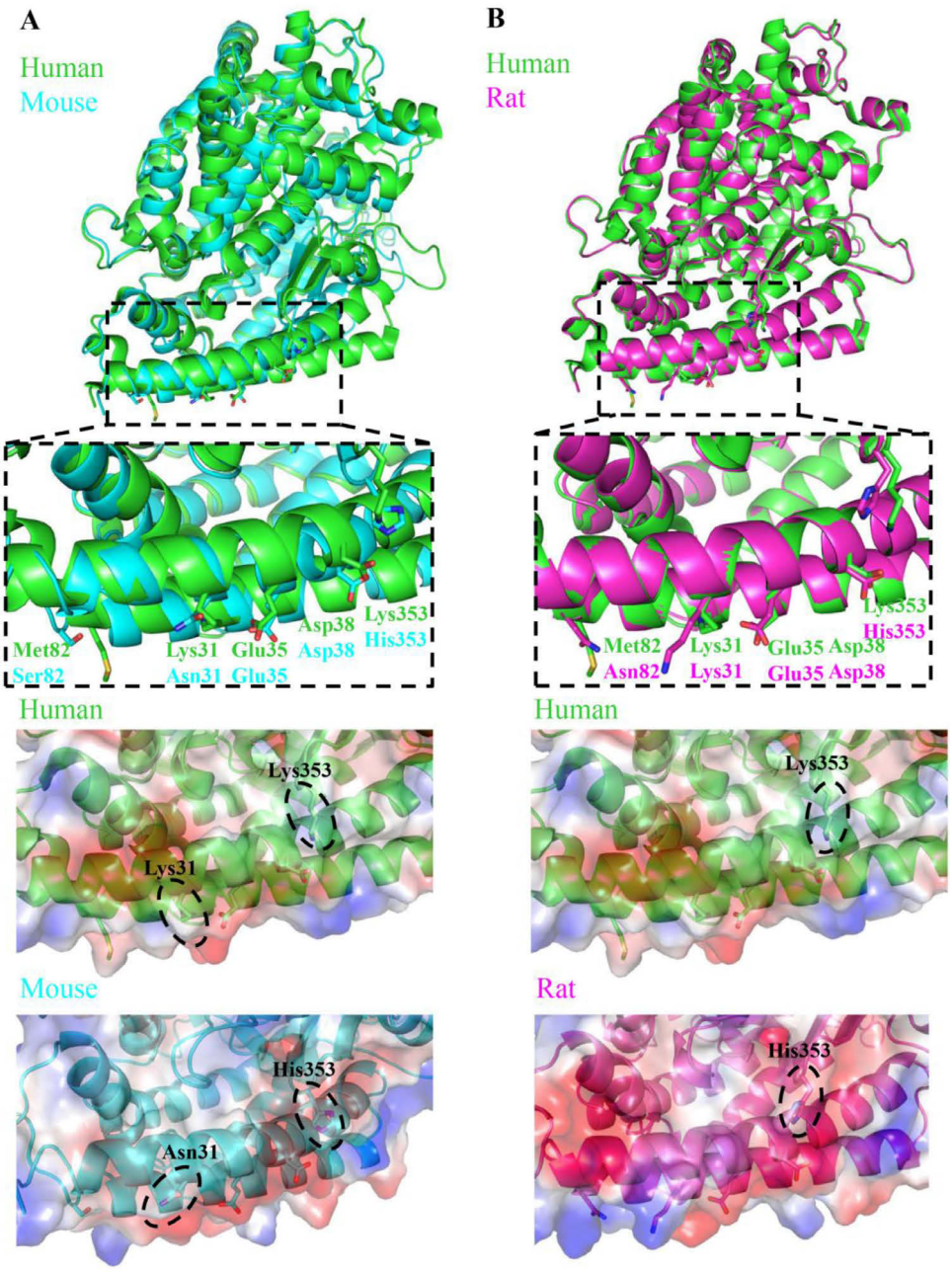

Fig. 2. Structural analyses of the human ACE2 (PDB code 2AJF) with the modeled mouse (A) and rat (B) ones in cartoon diagrams and surface electrostatic potential maps. The regions 30–41, 82–84 and 353–357 are enlarged and the critical residues are labeled. The changed ones affecting the electrostatic potential are labeled and circled in dashed lines. The electrostatic potential is colored from −62 to +62 kiloteslas/charge.

tribute to understanding cross-species receptor usage of this novel coronavirus.

Declaration of Competing Interest

The authors declare no conflict of interest.

Acknowledgments

This work was supported by Henan Emergency Project for Prevention and Control of 2019 Novel Coronavirus, the Earmarked Fund for Modern Agro-industry Technology Research System of China (CARS-35) and the Special Fund for Henan Agriculture Research System (S2012-06). The funders had no role in study design, data collection and interpretation, or the decision to submit the work for publication.

References

1. Wu F., Zhao S., Yu B., Chen Y.-.M., Wang W., Song Z.-.G., et al. A new coronavirus associated with human respiratory disease in China. *Nature* 2020 PubMed PMID:32015508 . doi:10.1038/s41586-020-2008-3.
2. Li Q., Guan X., Wu P., Wang X., Zhou L., Tong Y., et al. Early transmission dynamics in Wuhan, China, of novel coronavirus-infected pneumonia. *N Engl J Med* 2020 PubMed PMID:31995857 . doi:10.1056/NEJMoa2001316.
3. Li W., Moore M.J., Vasilieva N., Sui J., Wong S.K., Berne M.A., et al. Angiotensin–converting enzyme 2 is a functional receptor for the SARS coronavirus. *Nature* 2003;**426**(6965):450–4 PubMed PMID:14647384 .
4. Zhou P., Yang X.-.L., Wang X.-.G., Hu B., Zhang L., Zhang W., et al. A pneumonia outbreak associated with a new coronavirus of probable bat origin. *Nature* 2020 PubMed PMID:32015507. doi:10.1038/s41586-020-2012-7.

5. Letko M, Munster V. Functional assessment of cell entry and receptor usage for lineage b β-coronaviruses, including 2019-nCoV. bioRxiv. 2020:2020.01.22.915660.
6. Wan Y., Shang J., Graham R., Baric R.S., Li F.. Receptor recognition by novel coronavirus from Wuhan: an analysis based on decade-long structural studies of SARS. *J Virol* 2020 JVI.00127-20. PubMed PMID:31996437. eng.
7. Hulswit R.J.G., de Haan C.A.M., Bosch B.J.. Coronavirus spike protein and tropism changes. *Adv Virus Res* 2016;**96**:29–57 PubMed PMID:27712627. Epub 2016/09/13. eng.
8. Li F.. Structure, function, and evolution of coronavirus spike proteins. *Annu Rev Virol* 2016;**3**(1):237–61 PubMed PMID:27578435. Epub 2016/08/25. eng.
9. Li F., Li W., Farzan M., Harrison S.C.. Structure of sars coronavirus spike receptor-binding domain complexed with receptor. *Science* 2005;**309**(5742):1864–8 PubMed PMID:16166518. eng.
10. Li F.. Structural analysis of major species barriers between humans and palm civets for severe acute respiratory syndrome coronavirus infections. *J Virol* 2008;**82**(14):6984–91 PubMed PMID:18448527. Epub 2008/04/30. eng.

Rui Li, Songlin Qiao
Key Laboratory of Animal Immunology of the Ministry of Agriculture, Henan Provincial Key Laboratory of Animal Immunology, Henan Academy of Agricultural Sciences, Zhengzhou 450002, China

Gaiping Zhang*
Key Laboratory of Animal Immunology of the Ministry of Agriculture, Henan Provincial Key Laboratory of Animal Immunology, Henan Academy of Agricultural Sciences, Zhengzhou 450002, China
College of Animal Science and Veterinary Medicine, Henan Agricultural University, Zhengzhou 45002, China

*Corresponding author at: Key Laboratory of Animal Immunology of the Ministry of Agriculture, Henan Provincial Key Laboratory of Animal Immunology, Henan Academy of Agricultural Sciences, Zhengzhou 450002, China.
E-mail address: zhanggaip@126.com (G. Zhang)

Accepted 12 February 2020
Available online 21 February 2020

https://doi.org/10.1016/j.jinf.2020.02.013

Trend and forecasting of the COVID-19 outbreak in China

Dear Editor,

Very recently, a letter in Journal of Infection reported the outbreak of the novel cornonavirus from Dec. 2019 in China, especially in Hubei province.[1] This novel cornonavirus may originate from the bat,[2] is just named as the COVID-19 by the World Health Organization (WHO). The COVID-19 outbroke from Wuhan, the capital of Hubei province, has spread to other provinces of China and even other countries.[3] Strong human-to-human transmission is established.[4] Until Feb. 11, 2020, there have been 44653 cases of COVID-19 infections confirmed in mainland China, including 1113 deaths. To prevent and control the spread of the epidemic, many strategies are needed.[5] Predicting the trend of the epidemic are quite important to the allocation of medical resources, the arrangement of production activities, and even the domestic economic development all over China. Therefore, it is very urgent to use the latest data to establish an efficient and highly suitable epidemic analysis and prediction model according to the actual situation, and then to give reliable predictions, which could provide an important reference for the government to formulate emergency macroeconomic decisions and medical resources allocation.

Recently, the susceptible-exposed-infectious-recovered (SEIR) or other similar models[6,7] are used to forecast the potential domestic and international spread of this COVID-19 epidemic with parameters estimated from other sources.The real situation could be much more complicated and changing all the time. Especially, with the implementation of the Chinese government's multiple epidemic control policies, the control of nationwide epidemic has become obvious. However, the medical supplies in Hubei will still affect the implementation of national policies. In this letter, we present the current situation of the epidemic, predict the ongoing trend with data driven analysis, and estimate the outbreak size of the COVID-19 in both Hubei and other areas in mainland China.

The data of the epidemic are listed in Table 1 and also graphically shown in Fig. 1, in which "China" is used to denote the mainland China, and "Other" mainland China other than Hubei province. The data includes the daily confirmed(suspected) infections, totally confirmed(suspected) infections, daily deaths, and total deaths from Jan. 20, to Feb. 11, 2020, reported by the National Health Commission of the Republic of China (NHC),[8], and Health Commission of Hubei Province (HCH).[9] Jan. 20, 2020, containing all the cases reported from 0 to 24, is the zeroth day in this letter, and then others are implied. The total number of suspected cases reaches the peak value on the 19th day (Feb. 8), and then drops rapidly. Notice that, until Feb. 11, 2020, almost all the cases of deaths (1068/1113, 96%,) locates in Hubei province, which reveals the epidemic in Hubei is much more serious than that in the other areas of China. On the hand, it states the strict quarantine and limitation on population mobility have effectively prevented outbreaks in other provinces of China.

We use function $h(t) = A\left[(1+e^{-kx})^{-1} - (1+e^{k-kx})^{-1}\right]$ to describe the data of daily infections and deaths in Hubei, where $x = (t + 0.5 - t_T)$ with t denoting the day, and t_T representing the turning point; A and k are the parameters and determined by the data together with t_T. The cumulative data of infections or deaths are obtained by the integration over $h(t)$. For the epidemic in the other areas of China, the data of infections shows an asymmetric character, and then will be described as $s(t) = B\exp\left[-(x + k_1 e^{-x/k_1})\right]$, where $x = t - t_T$; the parameters B, k_1, and k_2 together with t_T, are then determined by fitting to the data.

Fig. 2 shows the fit and trend predictions to the total infections and deaths in Hubei and China other than Hubei. The extracted turning point of the infections in Hubei is the 17th day, namely, Feb. 6, 2020. The epidemic in Hubei is predicted to end after Mar. 10, 2020. We estimated that the epidemic is to end up with a total of 39, 000 infections in Hubei, not including the clinically diagnosed cases since Feb. 12, which may enlarge the prediction by 1.4 times. With considered data, namely, data from Jan. 20 to Feb. 11, the average errors are bout 166 and 190 for the fits to describe the daily and cumulative infections in Hubei, respectively, corresponding to 8.6% and 1.6% for the average relative errors, respectively.

Fig. 2 (b) and (e) shows the estimations of the total and daily deaths in Hubei. The predicted turning point is Feb. 12, 2020. The total deaths is estimated to be 2250. Notice the distribution of the daily deaths is delayed about 5∼6 days compared with the that of the daily infections. The average errors are bout 4 and 22 for the model to describe the daily and cumulative death numbers, respectively, corresponding to the relative errors 8.6% and 6.2%, respectively.

The numbers of the daily and total infections in China other than Hubei are showed in Fig. 2(c) and 2(f), respectively. The extracted turning point is Feb. 1, 2020 and the epidemic is expected to end on the 45th day, namely, on Mar. 5, 2020. The estimated number of cumulative infections is about 12,600 in China other

Table 1
The data of epidemic caused by the COVID-19 pneumonia in the mainland China and Hubei, including (A) daily infections, (B) daily deaths, (C) total infections, (D) total deaths, (E) daily and (F) total suspected cases.

Date	China						Hubei			
	A	B	C	D	E	F	A	B	C	D
2020/1/20	77	2	291	6	27	54	72	2	270	6
2020/1/21	149	3	440	9	26	37	105	3	375	9
2020/1/22	131	8	571	17	257	393	69	8	444	17
2020/1/23	259	8	830	25	680	1072	105	7	549	24
2020/1/24	444	16	1287	41	1118	1965	180	15	729	39
2020/1/25	688	15	1975	56	1309	2684	323	13	1052	52
2020/1/26	769	24	2744	80	3806	5794	371	24	1423	76
2020/1/27	1771	26	4515	106	2077	6973	1291	24	2714	100
2020/1/28	1459	26	5974	132	3248	9239	840	25	3554	125
2020/1/29	1737	38	7711	170	4148	12,167	1032	37	4586	162
2020/1/30	1982	43	9692	213	4812	15,238	1220	42	5806	204
2020/1/31	2102	46	11,791	259	5019	17,988	1347	45	7153	249
2020/2/1	2590	45	14,380	304	4562	19,544	1921	45	9074	294
2020/2/2	2829	57	17,205	361	5173	21,558	2103	56	11,177	350
2020/2/3	3235	64	20,438	425	5072	23,214	2345	64	13,522	414
2020/2/4	3887	65	24,324	490	3971	23,260	3156	65	16,678	479
2020/2/5	3694	73	28,018	563	5328	24,702	2987	70	19,665	549
2020/2/6	3143	73	31,161	636	4833	26,359	2447	69	22,112	618
2020/2/7	3399	86	34,546	722	4214	27,657	2841	81	24,953	699
2020/2/8	2656	89	37,198	811	3916	28,942	2147	81	27,100	780
2020/2/9	3062	97	40,171	908	4008	23,589	2618	91	29,631	871
2020/2/10	2478	108	42,638	1016	3536	21,675	2097	103	31,728	974
2020/2/11	2015	97	44,653	1113	3342	16,067	1638	94	33,366	1068

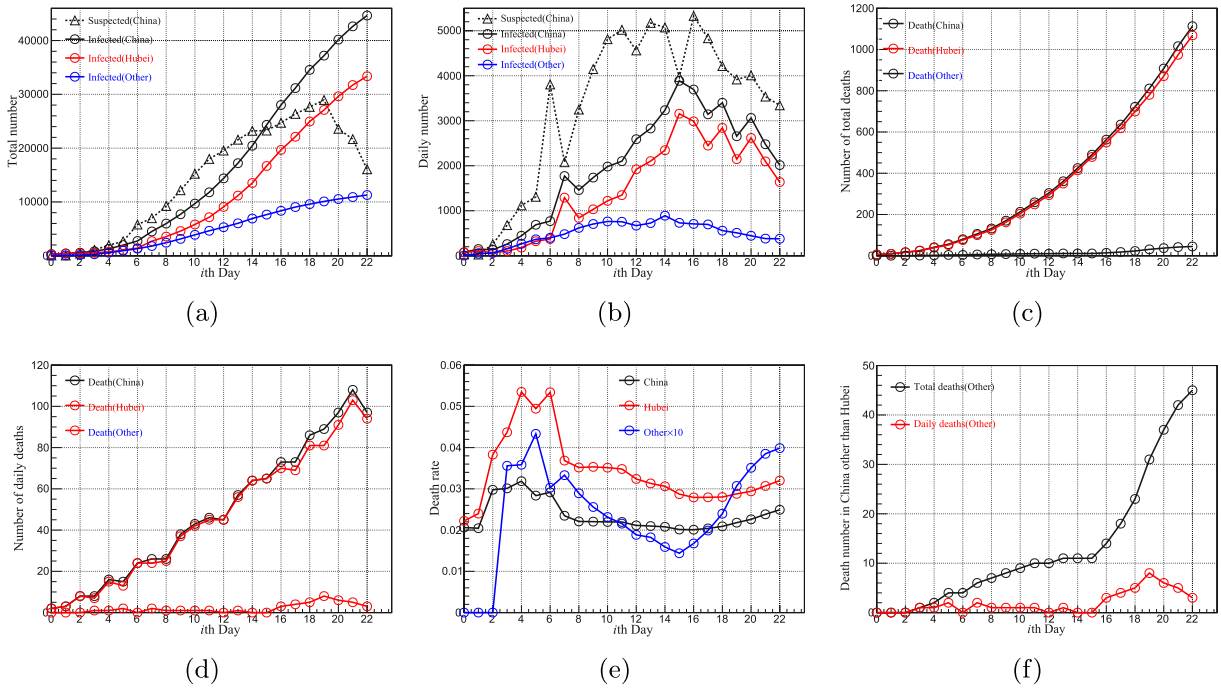

Fig. 1. Varies of the COVID-19 epidemic (Jan. 20–Feb. 11, 2020) in China, with (a) total and (b) daily suspected and confirmed cases, (c) total and (d) daily deaths, (e) death rate, and (f) deaths in China other than Hubei.

than Hubei. With the data in the considered period, the average errors are bout 41 and 58 for this model to describe the daily and total cumulative infections, and the corresponding relative errors are about 8.4% and 1.2%, respectively. Due to the minority of the statistical data in deaths of China other than Hubei (45 until Feb. 11, 2020, see Fig. 1(f)), we did not parameterize this data, and hence did not give a trend prediction.

The COVID-19 epidemic in China is predicted to end after Mar. 20, 2020, and cause 52,000–68,000 infections and about 2400 deaths. However, the data trends show that the quick and active strategies to reduce human exposure taken in China, such as limitation on population mobility and interpersonal contact rates, strict quarantine on migrants, have already had good impacts on control of the epidemic. Now the outbreak and deaths of the COVID-19 epidemic are mainly in Hubei province. After this letter has been written, the Hubei reported 14,840 confirmed infections (including 13,332 clinically diagnosed cases) on Feb. 12, 2020, which is almost 9 times greater than the data of the previous day. The huge fluctuation is due to the changing of diagnostic criteria in Hubei. And this clinical criteria taken in Hubei is expected to play an active and important role in controlling the outbreak and death rate.

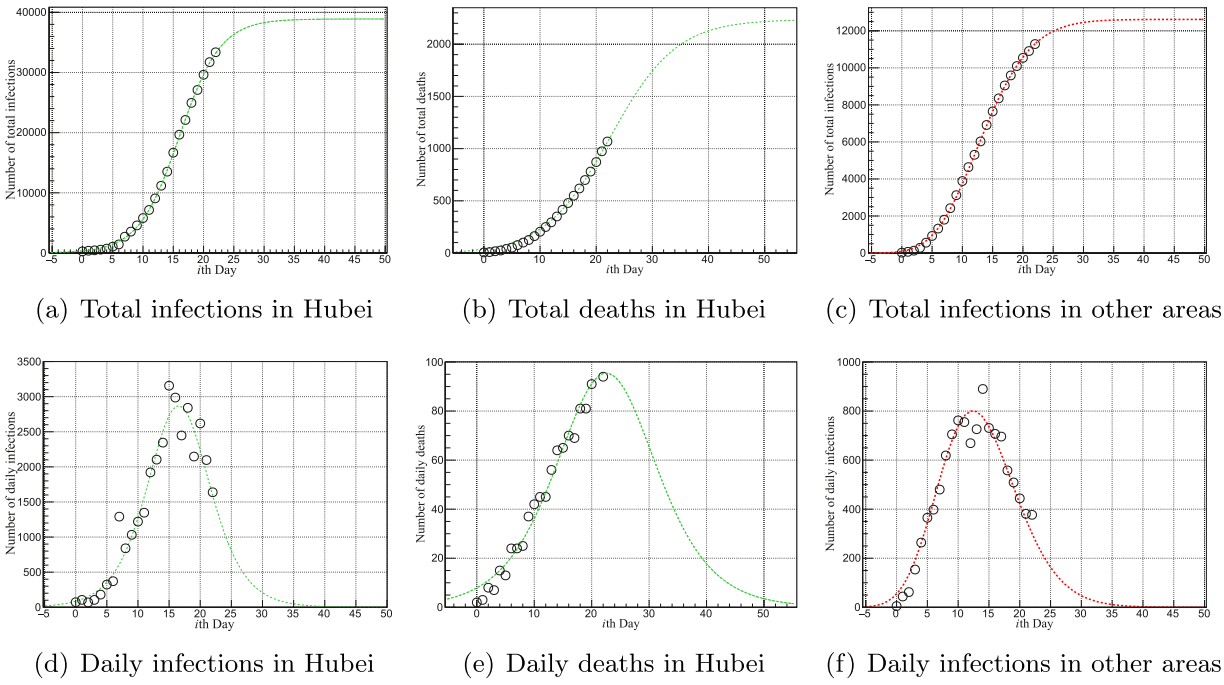

Fig. 2. Data (Jan. 20–Feb. 11, 2020) and fits of the infections and deaths in China; the black circle denotes the data, and the dotted line the predicted trend; the turning points of daily infections and deaths in Hubei are predicted to be Feb. 6, and Feb. 12, 2020, respectively, and Feb. 1 for daily infections in China other than Hubei.

Declaration of Competing Interest

The authors declare no conflict of interest.

Acknowledgments

We thank Jing Li and Hao-Nan Wang for the helpful discusses and suggestions. This work is supported by the Open Research Fund of Key Laboratory of Digital Earth Science (2019LDE005), and by the Fundamental Research Funds for the Central Universities under Grant No. 310201911QD054.

References

1. Wang R., Zhang X., Irwin D.M., Shen Y.. Emergence of SARS-like coronavirus poses new challenge in China. *J Infect* 2020. doi:10.1016/j.jinf.2020.01.017. Pii: S0163-4453(20)30057-8, [Epub ahead of print].
2. Li X., Song Y., Wong G., Cui J.. Bat origin of a new human coronavirus: there and back again. *Sci China Life Sci* 2020b;**13**.
3. C. Rothe, M. Schunk, P. Sothmann, G. Bretzel, G. Froeschl, C. Wallrauch, et al. Transmission of 2019-ncov infection from an asymptomatic contact in germany. N. Engl. J. Med. doi:10.1056/NEJMc2001468.
4. Q. Li, X. Guan, P. Wu, X. Wang, L. Zhou, Y. Tong, et al. Early transmission dynamics in wuhan, china, of novel coronavirus-infected pneumonia. *N. Engl. J. Med.* 2020a. Published online Jan. 29. DOI:10.1056/NEJMoa2001316
5. Wang F.-S., Zhang C.. What to do next to control the 2019-ncov epidemic? *The Lancet* 2020;**395**(10222):391–3.
6. J. T Wu, K. Leung, and G. M Leung. Nowcasting and forecasting the potential domestic and international spread of the 2019-ncov outbreak originating in Wuhan, China: a modelling study. *The Lancet* **395** (10225), 2020, 689-697. Online published (Jan. 31, 2020). doi:10.1016/S0140-6736(20)30260-9.
7. Tang B., Bragazzi N.L., Li Q., Tang S., Xiao Y., Wu J.. An updated estimation of the risk of transmission of the novel coronavirus (2019-ncov). *Infect Dis Model* 2020;**5**:248–55.
8. National Health Commission of People's Republic of China (2020). Outbreak notification. (in Chinese), Jan. 21, 2020-Feb. 13.
9. Health Commission of Hubei Province, (2020). Prevention and control of novel coronavirus pneumonia. Information release (in Chinese), Jan. 21, 2020-Feb. 13.

Qiang Li
School of Physical Science and Technology, Northwestern Polytechnical University, Xi'an 710129, PR China

Wei Feng*, Ying-Hui Quan
School of Electronic Engineering, Xidian University, Xi'an 710071, PR China

*Corresponding author.
E-mail addresses: liruo@nwpu.edu.cn (Q. Li), wfeng@xidian.edu.cn (W. Feng), yhquan@mail.xidian.edu.cn (Y.-H. Quan)

Accepted 20 February 2020
Available online 27 February 2020

https://doi.org/10.1016/j.jinf.2020.02.014

The potential threat of avian influenza virus to horses – Recalling the Chinese 1989–1990 equine influenza outbreaks

Dear Editor,

Recently, several studies in this journal have highlighted the threat of avian influenza virus (AIV) to humans, poultry, and other animals.[1–6] In equines, there was only one reported influenza outbreak caused by AIV, which occurred in 1989–1990 in China. However, AIV still poses a potential threat to equines.

In contrast to AIV, equine influenza virus (EIV) is a commonly known causative pathogen of acute respiratory disease in equines. To date, two subtypes of EIVs have been determined in the equine population worldwide: H7N7 and H3N8.[7] H7N7 EIV was initially identified in Prague in 1956, and the last outbreak caused by H7N7 EIV occurred in 1979.[7] H3N8 EIV was first isolated in Miami in 1963 and is currently responsible for EI outbreaks worldwide. During continuous transmission and evolution in equines, H3N8

EIV strains diverged genetically into three distinct lineages: pre-divergent, European, and American.[7]

Historically, there have been four main EI outbreaks in mainland China, occurring in 1974, 1989–1990, 1994, and 2007–2008. In the first, third, and fourth outbreaks, the isolated EIV strains were of the H7N7 subtype, H3N8 subtype European lineage, and H3N8 subtype American lineage, respectively. In the second EI outbreak, the causative pathogen (A/equine/Jilin/1/1989) was determined to be H3N8 subtype influenza A virus (IAV) by antigenicity characterization. However, after genetic sequencing, all eight segments of A/equine/Jilin/1/1989 were genetically closer to those of avian influenza virus than those of EIV, indicating an interspecies transmission event.

The 1989–1990 EI outbreaks in China contain two major outbreaks. The first EI outbreak occurred in Jilin and Heilongjiang Provinces between March and June 1989, with a morbidity of 81% and a mortality of up to 20% in some herds. The second EI outbreak occurred in Heilongjiang Province in April 1990, with a morbidity of 41% and no mortality. The high mortality and unique antigenicity of A/equine/Jilin/1/1989 attracted the attention of EIV researchers. However, after the 1989–1990 EI outbreaks in China, the virus disappeared from the equine population for unknown reasons.

Although no evidence in the epidemiological investigation worldwide supports the continuous circulation of A/equine/Jilin/1/1989-like EIV in equines, we should not underestimate the potential of interspecies AIV transmission to equines and the possibility of future EI outbreaks caused by AIV.

The haemagglutinin (HA) of IAVs recognizes and binds the cell surface sialic acid (SA) receptor of the host respiratory tract, and then the virus enters into cells and replicates. The distribution of the SA receptor influences the host range of IAVs. Human influenza viruses preferentially bind the SAa2,6 Gal receptor, while AIVs preferentially bind the SAa2,3 Gal receptor. It has been reported that the SAa2,3 Gal receptor is abundant in the epithelial cells of the horse trachea, and animal experiments indicate that IAVs with an HA recognizing the SAa2,3 Gal receptor could replicate in horses. This finding provides a prerequisite for cross-species transmission of AIV to equines.

In fact, there were several pieces of direct molecular evidence supporting the interspecies transmission of AIV to equines, in addition to the 1989–1990 EI outbreaks in China. In 2010, Abdel-Moneim et al. reported one H5N1 EIV strain (A/equine/Egypt/av1/2009) isolated from donkeys with cough, fever and serous nasal discharge in Egypt.[8] Sequencing results indicated that the virus had a close genetic relatedness to H5N1 AIV. In addition, H5 seroconversion was observed in 25.71% (27/105) of the examined donkeys. In 2011, He collected 284 equine lung tissue samples in China and isolated one AIV-derived H9N2 EIV strain (A/equine/Guangxi/3/2011) (https://kns.cnki.net/KCMS/detail/detail.aspx?dbcode=CMFD&dbname=CMFD201301&filename=1012496506.nh&v=MTMxMzc3ck5WRjI2SExleEdOVE1xWkViUElSOGVYMUx1eFlTN0RoMVQzcVRyV00xRnJDVVJMT2VaZVptRkNua1U=). Among the tested equine serum samples in China, 0.54% (7/1110) of samples were positive for anti-H9N2 antibody. In the 2015–2016 EI outbreaks in Pakistan, Khana et al. reported that the isolated EIV strain (A/equine/Pakistan/16) was reassorted from AIV.[9]

The common characteristic for the reported cross-species transmission events of AIV to equines in China, Pakistan, and Egypt is that they occur in farming equines.[8,9] In the mixed farming system, equines and domestic poultry often live in close proximity. Compared with racehorses, farming equines have more opportunities to contact domestic poultry and experience long-term environmental exposure to poultry. AIV infections in poultry increase exposure risks to equines. Recently, frequent reports of cross-species transmission events of AIV to farming dogs in China and Korea also indicate the potential threat of AIV to farming animals with close contact with poultry.[10]

Another problem is that the farming equines in China, Pakistan, and Egypt had no vaccination history. Even in some racehorse populations, vaccinations for EIV are not routinely performed as recommended by the World Organization for Animal Health (OIE) Expert Surveillance Panel on EI vaccine composition. Although H3N8 EIV is antigenically distinct from A/equine/Jilin/1/1989, animal experiments indicated that high doses of EI vaccines still provided complete protection against challenge with A/equine/Jilin/1/1989. Accordingly, routine vaccination with H3N8 EI vaccines in equines might prevent AIV infection to some degree, at least for H3N8 subtype AIV.

Several strategies may help reduce the threat of AIV to equines, including reducing exposure of equines to poultry, birds, and other hosts of IAV, especially animals with clinical signs of influenza virus infection; monitoring AIV prevalence in domestic poultry around equines and routinely vaccinating domestic poultry with AIV vaccines; vaccinating susceptible equines with EI vaccines, especially farming equines in close contact with domestic poultry; and monitoring the prevalence of multiple AIV subtypes in equines, not merely that of those restricted to H3N8 subtype.

Declaration of Competing Interest

None.

Acknowledgments

This work was supported by the National Natural Science Foundation of China (31702271) and the Guangdong Provincial Natural Science Foundation (2017A030310367).

References

1. Zhang W.Y., Zhao K.F., Jin J., He J., Zhou W., Wu J.J., et al. A hospital cluster combined with a family cluster of avian influenza H7N9 infection in Anhui province, China. *J Infect* 2019;**79**:49–55.
2. Tong X.C., Weng S.S., Xue F., Wu X., Xu T.M., Zhang W.H., et al. First human infection by a novel avian influenza A(H7N4) virus. *J Infect* 2018;**77**:255–7.
3. Teng Y., Bi D.H., Guo X.C., Hu D.W., Feng D., Tong Y.G., et al. Contact reductions from live poultry market closures limit the epidemic of human infections with H7N9 influenza. *J Infect* 2018;**76**:295–304.
4. Yang Y., Wong G., Yang L.Q., Tan S.G., Li J.M., Bai B., et al. Comparison between human infections caused by highly and low pathogenic H7N9 avian influenza viruses in wave five: clinical and virological findings. *J Infect* 2019;**78**:241–8.
5. Kang Y.F., Shen X.J., Yuan R.Y., Xiang B., Fang Z.X., Murphy R.W., et al. Pathogenicity and transmissibility of three avian influenza A (H5N6) viruses isolated from wild birds. *J Infect* 2018;**76**:286–94.
6. Li T.G., Ma Y., Li K.B., Tang X.P, Wang M., Yang Z.C., et al. Death of a very young child infected with influenza A (H5N6). *J Infect* 2016;**73**:626–7.
7. Cullinane A., Newton J.R.. Equine influenza-A global perspective. *Vet Microbiol* 2013;**167**:205–14.
8. Abdel-Moneim A.S., Abdel-Ghany A.E., Shany S.A.. Isolation and characterization of highly pathogenic avian influenza virus subtype H5N1 from donkeys. *J Biomed Sci* 2010;**17**:25.
9. Khan A., Mushtaq M.H., Ahmad M.U.D., Nazir J., Farooqi S.H., Khan A.. Molecular epidemiology of a novel re-assorted epidemic strain of equine influenza virus in Pakistan in 2015–16. *Virus Res* 2017;**240**:56–63.
10. Su S., Li H.T., Zhao F.R., Chen J.D., Xie J.X., Z.M. Chen, et al. Avian-origin H3N2 canine influenza virus circulating in farmed dogs in Guangdong, China. *Infect Genet Evol: J Mol Epidemiol Evol Genet Infect Dis* 2013;**14**:444–9.

Jiajun Ou[1]
College of Veterinary Medicine, South China Agricultural University, Guangzhou, 510642 Guangdong Province, China
Guangdong Provincial Key Laboratory of Prevention and Control for Severe Clinical Animal Diseases, Guangzhou, 510642 Guangdong Province, China
Guangdong Technological Engineering Research Center for Pet, Guangzhou, 510642 Guangdong Province, China

Mian Huang[1], Xuanjiao Chen
Guangzhou Zoo, Guangzhou, 510642 Guangdong Province, China

Zengchao Wang, Gang Lu*, Shoujun Li*
College of Veterinary Medicine, South China Agricultural University, Guangzhou, 510642 Guangdong Province, China
Guangdong Provincial Key Laboratory of Prevention and Control for Severe Clinical Animal Diseases, Guangzhou, 510642 Guangdong Province, China
Guangdong Technological Engineering Research Center for Pet, Guangzhou, 510642 Guangdong Province, China

*Corresponding authors at: College of Veterinary Medicine, South China Agricultural University, Guangzhou, 510642 Guangdong Province, China.
E-mail addresses: lg@scau.edu.cn (G. Lu), shoujunli@scau.edu.cn (S. Li)

[1] These authors contributed equally to this study.
Accepted 23 December 2019
Available online 28 December 2019

https://doi.org/10.1016/j.jinf.2019.12.013

Cerebrospinal fluid MinION sequencing of 16S rRNA gene for rapid and accurate diagnosis of bacterial meningitis

Dear Editor,

We read with interest recent articles in this journal regarding the utility of next-generation sequencing for the diagnosis bacterial meningitis.[1,2] Bacterial meningitis causes substantial morbidity and mortality worldwide.[3] Rapid identification of the microorganisms is essential for early initiation of appropriate antimicrobial therapy, thereby improving clinical outcome. Yet routine diagnostic methods fail to identify the bacteria in the majority of patients. Over the last decade, advanced sequencing technologies have greatly improved our capacity to detect the causative agents of infectious diseases in clinical samples.[4,5] Of these, the single molecule real-time sequencing developed by Oxford Nanopore Technologies (ONT) is a promising tool for diagnostic setting because of its short turnaround time.

In late April 2019, a 59-year old seller of fish-noodles was referred to our hospital with a 1-day history of headache, fever and vomiting. He had a history of heavy alcohol use and hepatitis C infection, and had cirrhosis and diabetes mellitus. On admission, he was unconsciousness (a Glasgow Coma Scale of 8), with a body temperature of 40 °C, a blood pressure of 140/80 mmHg and neck stiffness. Initial Gram-stain and microscopy of CSF showed Gram-positive cocci, 8449 white cells/uL with 91% neutrophils, elevated protein and low glucose level, and high lactate concentration (Fig. 1A). Routine bacterial culture, plus *Streptococcus pneumoniae* and *S. suis* PCRs were all negative. He was diagnosed with bacterial meningitis, and given a combination of ceftriaxone (2 g/12 h) and dexamethasone (0.4 mg/kg/12 h). His clinical condition steadily improved. His second and third CSF samples became negative by Gram stain. The other CSF parameters also improved, except the glucose, which remained low (Fig. 1A). On day 20 of hospitalization, the patient suddenly became unconsciousness with fever. Brain magnetic resonance imaging showed bifrontal abscesses (Fig. 1B). After consulting a local neurosurgeon, aspiration of the brain abscesses was not advised and the patient was treated empirically with meropenem (2 g/8 h) and vancomycin (1 g/8 h). Due to continued diagnostic uncertainty, we performed 16S rRNA sequencing of the admission CSF, stored as part of an going clinical study (Supplementary Materials), using an established Sanger-sequencing based 16S rRNA method.[6] Subsequently, analysis of the obtained sequences revealed evidence of *S. agalactiae* (Supplementary Figure 1). Given this new diagnostic result of the admission CSF and because the patient had recovered clinically, the patient was given 24 million units of penicillin G for every 4 h. After day 43 of hospitalization, all CSF parameters had normalised (Fig. 1A). Likewise, on CT scan the brain abscess was now significantly improved (Fig. 1C). The patient was discharged with full clinical recovery.

Additionally, MinION sequencing of complete 16S rRNA gene was retrospectively carried out on the extracted nucleic acid of the admission CSF yielded a total of 14,848 reads after 100 min of sequencing run. Of these, 11,556 reads (79%) were successfully aligned to *S. agalactiae* (Fig. 1D). The remaining reads were assigned to other Streptococcus species (mostly *S. dysgalacticiae* ($n = 2.145$, 14%)), likely attributed to a combination of the high level of sequence similarities of the 16S rRNA region between them and the sequencing errors introduced by the MinION systems. Analysis of sequencing data generated during the 25, 50 and 75 min of sequencing run time also yielded the same results (Supplementary Figure 2). Details about the MinION procedure are presented in Supplementary Materials.

To further assess of the utility of CSF MinION sequencing of 16S rRNA gene for the detection of bacterial meningitis pathogens, six CSF samples from patients with confirmed bacterial meningitis enrolled in the abovementioned clinical study were tested (Table 1). Analysis of the MinION reads obtained after two hours of the sequencing run showed that the majority of reads were correctly assigned to the corresponding bacterial species (*S. pneumoniae* and *S. suis)* or genus (*Neisseria*) found in the CSF samples by diagnostic work up of the clinical study (Fig. 1E and Table 1). Additional analysis of the obtained reads generated at two earlier time points (20 min and 60 min) of the sequencing run generated the same results (Table 1).

Collectively, we report the first application of MinION sequencing of 16S rRNA gene to detect bacterial meningitis causing pathogens in CSF samples from a low and middle-income country. The assay was able to detect the bacterial causes in all of the seven tested CSF samples. Meanwhile, Gram stain and culture, the two most commonly used methods in clinical microbiology laboratories worldwide, were negative in 3/7 samples. (Fig. 1 and Table 1).

In addition to CSF samples described in the present study and a recent pilot study from Korea,[7] successful detections of *Haemophilus influenzae* in sputum and *Campylobacter fetus* in culture materials by MinION sequencing of 16S rRNA have recently been reported.[8] Together, the data suggest that MinION sequencing of 16S rRNA is a sensitive method for rapid and accurate detection of pan-bacterial pathogens, including unexpected microorganisms, in clinical samples. Additionally, the bacterial species information generated by the analysis of 16S rRNA sequences can be useful for disease surveillance and vaccine evaluation. Thus, the application of the method would be relevant for both patient management and epidemiological research. Indeed, to the best of our knowledge the present study represents the first report of *S. agalactiae* associated meningitis in Vietnam. Because the incidence of invasive diseases (including meningitis) caused by *S. agalactiae* has been reported with increased frequency in recent years,[9] *S. agalactiae* should be considered as an important differential

A

	Admission CSF	Second CSF	Third CSF	Fourth CSF
White cells, cells/uL	8449	21109	210	9
Neutrophils, %	91	78	73	33
Lymphocytes, %	9	22	27	67
Red cells, cells/uL	3000	11000	22	0
Protein, g/L	8.8	3.8	1	0.55
CSF glucose, mmol/L	3.3	3.4	3.4	3.28
Blood glucose, mmol/L	11.8	16	12.3	5.2
CSF/blood glucose ratio	0.28	0.21	0.28	0.63
Lactate, mmol/L	15	10	4.2	2.76
CSF appearance	Cloudy	Dark yellow	Colorless	Colorless
Lumbar puncture opening pressure, cmH2O	27	9	14	NA

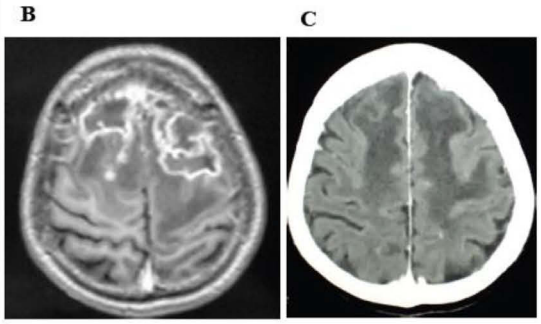

D

Taxon	Cumulative Reads
Streptococcus agalactiae	11,556
Streptococcus dysgalactiae	2,145
Streptococcus tangierensis	127
Streptococcus iniae	93
Streptococcus porcinus	73
Streptococcus cameli	72
Streptococcus suis	70
Streptococcus phocae	45
Streptococcus mitis	40
Streptococcus parasanguinis	38
Streptococcus canis	30
Streptococcus saliviloxodontae	30

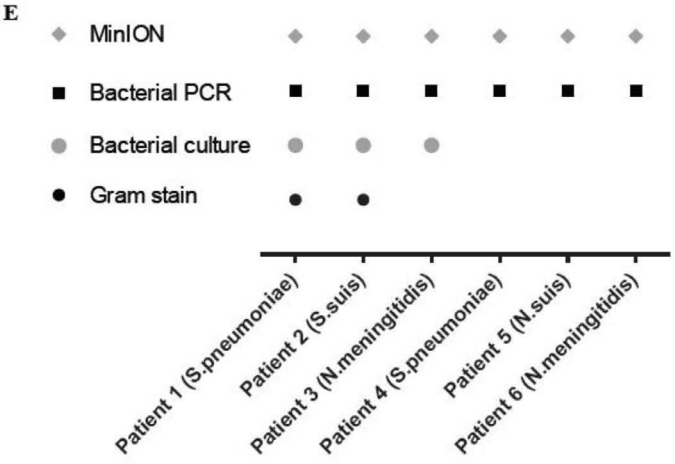

Fig. 1. Clinical profile of the *S. agalactiae* patient, and result of CSF MinION sequencing of 16S rRNA gene. (A) results of CSF investigations over the course of illness; (B) MRI showing bifrontal brain abscesses; (C) follow-up CT scan performed on 5th June 2019 showing the improvement of the brain abscesses; (D) results of MinION sequencing of the admission CSF samples taken on 25th April 2019. A total of 14,848 reads were obtained after 100 min of the sequencing procedure, of which1,556 (78%) reads were successfully aligned *S. agalactiae*; (E) result of MinION sequencing of 16S rRNA gene analysis of the six additional CSF samples alongside routine diagnostic yields. The appearances of specific symbols indicate the success of the corresponding methods in detecting the pathogens in the tested samples.
Note to Figure 1: The sampling dates of the second, third and fourth CSF samples were 27th April 2019, 17th May 2019, and 5th June 2019, respectively.

diagnosis for patients presenting with acute CNS infections in Vietnam.

Owing to the unavailability of the reagents at the time of patient admission, we were not able to perform real-time diagnosis using MinION sequencing on the collected CSF samples. However, same day diagnosis is theoretically achievable, because the current workflow takes 5 – 6 h to operate. Prospective study is urgently needed to assess its translational potential in the diagnosis of bacterial meningitis.

The clinical study

Since September 2017, a prospective observational study aiming at exploring the utility potential of next-generation sequencing in patients presenting with central nervous system (CNS) infections has been conducted in the brain infection ward of the Hospital for Tropical Diseases (HTD) in Ho Chi Minh City, Vietnam. HTD is a tertiary referral hospital for patients with infectious diseases from southern provinces of Vietnam, serving a population of >40 million. Any patient (≥16 years) with an indication for lumbar puncture was eligible for enrolment. Patient was excluded if no written informed consent was obtained. As per the study protocol, CSF, plasma and urine samples were collected at presentation alongside demographic, meta-clinical data and results of routine diagnosis. After collection, all clinical specimens were stored at −80 °C until analysis.

The clinical study received approvals from the Institutional Review Board of the HTD and the Oxford Tropical Research Ethics Committee of the University of Oxford. Written informed consent was obtained from each study participant or relative (if the patient was unconsciousness).

MinION sequencing of 16S rRNA

Sequencing of complete 16S rRNA gene was retrospectively performed using MinION Nanopore sequencer (ONT), following the manufacturer's instructions. In brief, amplification of the complete 16S rRNA gene and library preparation were carried out on extracted nucleic acid using 16S Barcoding Kit (SQK-RAB204, ONT) and primers (27F 5′-AGAGTTTGATCCTGGCTCAG-3′ and 1492R 5′-GGTTACCTTGTTACGACTT-3′), followed by the sequencing of the amplified product using R9.4 Flow cells (ONT). MinION reads were first basecalled using Albacore v2.1.7 (ONT), followed by demultiplexing using Porechop (https://github.com/rrwick/Porechop). Determination of bacterial genus/species composition in the obtained reads was then carried out using Epi2Me interface (Metrichor, Oxford, UK), a platform for cloud-based analysis of MinION data. Overall, the whole procedure of MinION sequencing of 16S rRNA gene takes 5–6 h to complete (Supplementary Figure 3).

Table 1
Demographics and clinical outcome of the additional six patients included for MinION Nanopore sequencing analysis of 16S rRNA gene.

	Patient 1	Patient 2	Patient 3	Patient 4	Patient 5	Patient 6
Demographics						
Age (years)	33	65	23	29	53	41
Gender	Male	Male	Female	Male	Male	Female
Origin	BP	BT	BP	NT	BT	TN
Illness day at enrollment (days)	5	3	1	15	4	2
Length of hospital stay (days)	17	5	12	15^	13	15
Clinical signs/symptoms						
Body temperature (°C)	37	38	38	37	37.2	37
Cranial nerve palsy	N	N	N	Y	N	N
Hemiplegia/paresis	N	N	N	N	N	N
Paraplegia/paresis	N	N	N	N	N	N
Tetraplegia/paresis	N	N	N	N	N	N
Generalized convulsions	N	N	N	N	N	N
Localized convulsions	N	N	N	N	N	N
Neck stiffness	Y	Y	Y	Y	Y	N
GCS at enrolment	14	14	13	13	9	12
CSF examinations						
CSF white cell counts	51,810	1609	3111	1126	16,744	4760
CSF neutrophils (%)	78	95	94	60	65	88
CSF lymphocytes (%)	22	5	6	40	35	12
CSF/blood glucose ratio	0.11	0.64	0.014	0.42	0.32	0.028
CSF lactate	11.4	9.21	12.45	5.82	13.94	15.62
Total protein	1.33	1.133	4.731	1.37	3.861	5.746
Routine microbial investigations						
ZN smear	ND	ND	Negative	Negative	ND	ND
India Ink stain	Negative	ND	Negative	Negative	ND	ND
Cryptococcal antigen test	ND	ND	ND	Negative	ND	ND
Gram stain	Gram-positive cocci	Gram-positive cocci	Negative	Negative	Negative	Negative
Bacterial culture	*S. pneumoniae*	*S. suis*	*N. meningitidis*	Negative	Negative	Negative
Bacterial PCR	*S. pneumoniae*	*S. suis*	*N. meningitidis*	*S. pneumoniae*	*S. suis*	*N. meningitidis*
MinION 16S rRNA sequencing						
20 min	*S. pneumoniae*	*S. suis*	*Neisseria*	*S. pneumoniae*	*S. suis*	*Neisseria*
1 h	*S. pneumoniae*	*S. suis*	*Neisseria*	*S. pneumoniae*	*S. suis*	*Neisseria*
2 h	*S. pneumoniae*	*S. suis*	*Neisseria*	*S. pneumoniae*	*S. suis*	*Neisseria*
GCS at discharge	15	14	15	14	14	15

Notes to Table 1: GCS: Glasgow Coma Score, BT: Ben Tre, BP: Binh Phuoc, TN: Tay Ninh, NT: Ninh Thuan, HCMC: Ho Chi Minh City, BM: bacterial meingitis, TBM: tuberculous meningitis; N: no, Y: yes; ND: not done.

Declaration of Competing Interest

We, the author of the submitted manuscript declare that we do not have a commercial or other association that might pose a conflict of interest (e.g., pharmaceutical stock ownership, consultancy, advisory board membership, relevant patents, or research funding).

Acknowledgments

We thank Le Kim Thanh, Le Nguyen Truc Nhu, and Lam Anh Nguyet for their logistic support. We are indebted to patients for their participations in this study.

This study was funded by the Wellcome Trust of Great Britain (106680/B/14/Z and 204904/Z/16/Z).

Supplementary materials

Supplementary material associated with this article can be found, in the online version, at doi:10.1016/j.jinf.2019.12.011.

References

[1]. Guo L.Y., Li Y.J., Liu L.L., Wu H.L., Zhou J.L., Zhang Y., et al. Detection of pediatric bacterial meningitis pathogens from cerebrospinal fluid by next-generation sequencing technology. *J Infect* 2019;**78**(4):323–37.
[2]. Zhang J.Z., Zheng P., Sun H.M., Dong J.J., Li S.L., Fan S.Y., et al. Next-generation sequencing combined with routine methods to detect the pathogens of encephalitis/meningitis from a chinese tertiary pediatric neurology center. *J Infect* 2019;**78**(5):409–21.
[3]. Costerus J.M., Brouwer M.C., Bijlsma M.W., van de Beek D.. Community-acquired bacterial meningitis. *Curr Opin Infect Dis* 2017;**30**(1):135–41.
[4]. Kai S., Matsuo Y., Nakagawa S., Kryukov K., Matsukawa S., Tanaka H., et al. Rapid bacterial identification by direct pcr amplification of 16S rRNA genes using the MinION™ nanopore sequencer. *FEBS Open Bio* 2019;**9**(3):548–57.
[5]. Moon J., Kim N., Lee H.S., Shin H.R., Lee S.T., Jung K.H., et al. Campylobacter fetus meningitis confirmed by a 16S rRNA gene analysis using the MinION nanopore sequencer, South Korea, 2016. *Emerg Microbes Infect* 2017;**6**(11):e94.
[6]. Tytgat B., Verleyen E., Obbels D., Peeters K., De Wever A., D'Hondt S., et al. Bacterial diversity assessment in antarctic terrestrial and aquatic microbial mats: a comparison between bidirectional Pyrosequencing and cultivation. *PLoS One* 2014;**9**(6):e97564.
[7]. Moon J., Kim N., Kim T.J., Jun J.S., Lee H.S., Shin H.R., et al. Rapid diagnosis of bacterial meningitis by nanopore 16S amplicon sequencing: a pilot study. *Int J Med Microbiol* 2019;**309**(6):151338.
[8]. Moon J., Jang Y., Kim N., Park W.B., Park K.I., Lee S.T., et al. Diagnosis of haemophilus influenzae pneumonia by nanopore 16S amplicon sequencing of sputum. *Emerg Infect Dis* 2018;**24**(10):1944–6.
[9]. Francois Watkins L.K., McGee L., Schrag S.J., Beall B., Jain J.H., Pondo T., et al. Epidemiology of invasive group b streptococcal infections among nonpregnant adults in the united states, 2008-2016. *JAMA Intern Med* 2019;**179**(4):479–88.

Nguyen Thi Thu Hong
Oxford University Clinical Research Unit, Ho Chi Minh City, Vietnam

Ho Dang Trung Nghia
Oxford University Clinical Research Unit, Ho Chi Minh City, Vietnam
Pham Ngoc Thach University of Medicine, Ho Chi Minh City, Vietnam
Hospital for Tropical Diseases, Ho Chi Minh City, Vietnam

Tran Tan Thanh
Oxford University Clinical Research Unit, Ho Chi Minh City, Vietnam

Nguyen Phu Huong Lan

Hospital for Tropical Diseases, Ho Chi Minh City, Vietnam

Nguyen Thi Han Ny
Oxford University Clinical Research Unit, Ho Chi Minh City, Vietnam

Nghiem My Ngoc
Hospital for Tropical Diseases, Ho Chi Minh City, Vietnam

Vu Thi Ty Hang
Oxford University Clinical Research Unit, Ho Chi Minh City, Vietnam

Le Thi My Chau, Van Xuan Quynh
Hospital for Tropical Diseases, Ho Chi Minh City, Vietnam

Le Thi Diem
Department of Medicine, Vietnam National University, Ho Chi Minh City, Vietnam

Bui Thi Bich Hanh
Pham Ngoc Thach University of Medicine, Ho Chi Minh City, Vietnam

Nguyen Ho Hong Hanh
Department of Medicine, Vietnam National University, Ho Chi Minh City, Vietnam

Du Trong Duc
Pham Ngoc Thach University of Medicine, Ho Chi Minh City, Vietnam

Dinh Nguyen Huy Man
Hospital for Tropical Diseases, Ho Chi Minh City, Vietnam

James Campbell
Oxford University Clinical Research Unit, Ho Chi Minh City, Vietnam
Centre for Tropical Medicine and Global Health, Nuffield Department of Medicine, University of Oxford, Oxford, United Kingdom

Pham Kieu Nguyet Oanh
Hospital for Tropical Diseases, Ho Chi Minh City, Vietnam

Jeremy Day
Oxford University Clinical Research Unit, Ho Chi Minh City, Vietnam
Centre for Tropical Medicine and Global Health, Nuffield Department of Medicine, University of Oxford, Oxford, United Kingdom

Nguyen Hoan Phu
Oxford University Clinical Research Unit, Ho Chi Minh City, Vietnam
Department of Medicine, Vietnam National University, Ho Chi Minh City, Vietnam

Nguyen Van Vinh Chau
Hospital for Tropical Diseases, Ho Chi Minh City, Vietnam

Guy Thwaites
Oxford University Clinical Research Unit, Ho Chi Minh City, Vietnam
Centre for Tropical Medicine and Global Health, Nuffield Department of Medicine, University of Oxford, Oxford, United Kingdom

Le Van Tan*
Oxford University Clinical Research Unit, Ho Chi Minh City, Vietnam

*Corresponding author.
E-mail address: tanlv@oucru.org (L.V. Tan)

Accepted 23 December 2019
Available online 28 December 2019

https://doi.org/10.1016/j.jinf.2019.12.011

Severe influenza a cases requiring extra-corporeal membrane oxygenation (ECMO) therapy, 2018–2019

Dear Editor,

Several aspects of influenza have been highlighted recently, including its global, comparative seasonality,[1] and issues around rapid point-of-care testing.[2] In addition, the UK has a national surveillance programme, the UK Severe Influenza Surveillance System (USISS) to monitor and investigate severe cases of influenza across the country,[3] including severe cases of influenza admitted to intensive care (ICU) and high dependency units (HDU).[4] Specifically, the aim of this latter arm was to "monitor and estimate the impact of seasonal influenza on the population" and to "describe the epidemiology of severe disease." This surveillance began in the 2011–2012 influenza season and has continued to the present, with mandatory participation by all NHS Trusts.

Leicester is one of 5 NHS commissioned centres in the UK providing extra-corporeal membrane oxygenation (ECMO) support for severe acute respiratory failure in adults. This process involves draining deoxygenated venous blood from the superior and inferior vena cavae, pumping this blood through a membrane lung, where oxygenation and carbon dioxide elimination take place. Oxygenated blood is delivered back into the right atrium, therefore replacing the function of the native lung. In this way, ECMO can be used to support patients with respiratory failure of any cause. Acceptance for admission for ECMO support follows referral to the ECMO service via structured questionnaire and discussion with the ECMO consultant on-call. Patients are commenced on ECMO where benefits are deemed to outweigh the risks in patients with potentially reversible respiratory failure, who are already on maximal conventional therapy at their referring centre, and who are not achieving lung protective ventilation.[5]

Here, as part of our national USISS role, we describe severe influenza cases that required ECMO support in whom the predominant indications were severe hypoxia with a PaO_2:FiO_2 ratio of <100 despite maximal conventional therapy, and/or hypercapnoeic respiratory failure with a pH <7.2 despite ventilation pressures >30 cm H_2O.

During the 2018–2019 influenza season 33 cases of severe influenza were admitted to Glenfield Hospital for ECMO from our referring centres. Most were male (23/33, 69.7%, 28–62 years, BMI: 17–47; female 10/33, 27–51 years, BMI: 21–38), and of white British ethnicity (30/33, 91.0%; with 1 each of Chinese, Asian, African ethnicity). Comorbidities included, obesity, hypertension, asthma, COPD, diabetes, anxiety, depression, epilepsy, a history of smoking and alcohol use (or abuse). All cases except for one influenza A(H3N2) infection (possibly two as subtyping was not performed for another sample) were due to influenza A(H1N1)pdm09. Only one case had a history of influenza vaccination. Various 'on referral' ECMO-related parameters were extracted, as well as contemporaneous laboratory results. These were statistically compared between patients who died ($n=8$) and those who survived using *t*-test or Mann-Whitney test for continuous variables and Fisher-exact test for categorical variables. Correlation between duration on ECMO and laboratory parameters was assessed using Spearman's rank correlation coefficient. ($n=24$) (Tables 1 and 2).

Surprisingly, it was found that on direct comparison, most of the referral parameters for patients starting ECMO were not statistically different between those influenza-infected patients that eventually survived ($n=24$) versus those who died ($n=8$) – a case fatality rate of 25%. One patient was dropped from this analysis due to some missing data.

Only the respiratory rate (RR, $p=0.041$) and the lactate ($p=0.008$) showed statistically significant differences between the two groups, with higher values being found in the patients who

Table 1
Admission characteristics between patients who survived versus those who died undergoing ECMO for severe influenza infection. Continuous data are expressed as means (SD) or medians (Q1, Q3) where appropriate, and categorical data as n (percentage).

Demographic/medical conditions	Survived ($n=24$)	Died ($n=8$)	p-value
Age (years)	42.8 (11.8)	46.4 (5.4)	0.261
Gender (male)	17 (70.8%)	5 (62.5%)	0.681
Ethnicity (white)	23 (95.8%)	7 (87.5%)	0.444
Body Mass Index	29.7 (6.2)	34.0 (10.3)	0.184
Influenza vaccinated	1 (4.2%)	0 (0.0%)	0.999
Smoker	4 (16.7%)	2 (25.0%)	0.625
Hypertension	4 (16.7%)	2 (25.0%)	0.625
Asthma	3 (12.5%)	1 (12.5%)	0.999
Clinical characteristics			
SOFA score	8.0 (2.9)	9.4 (2.6)	0.234
PaO_2:FiO_2 ratio	10.0 (4.1)	9.8 (2.2)	0.887
PEEP (cm H_20)	12 (11 - 15)	15 (14 - 15)	0.208
Tidal volume (mL)	486.7 (125.1)	468.8 (74.1)	0.709
Respiratory rate (RR, bpm)	**19.2 (5.8)**	**25.1 (8.1)**	**0.041**
Peak RR (bpm)	29.0 (3.4)	31.4 (8.6)	0.470
pH	7.3 (0.2)	7.3 (0.1)	0.618
PaO_2 (kPa)	8.2 (1.7)	8.9 (2.3)	0.318
$PaCO_2$ (kPa)	7.8 (3.2)	7.7 (1.5)	0.933
Base excess (mmol/L)	−0.9 (6.5)	−0.7 (8.4)	0.940
Lactate (mmol/L)	**1.5 (1.1 - 2.1)**	**2.7 (1.7 - 4.2)**	**0.008**
Bicarbonate (HCO_3, mmol/L)	24.1 (5.7)	24.1 (6.1)	0.986
C-reactive protein (mg/L)	240.3 (116.3)	281.2 (178.9)	0.507
White cell count (x10^9/L)	6.5 (3.7)	4.7 (6.0)	0.294
Haemoglobin (g/L)	126.1 (21.1)	127.8 (32.0)	0.873
Platelets (x10^9/L)	202.7 (111.1)	143.6 (75.5)	0.174
ALT (IU/L)	57.5 (38.5 - 101.5)	31 (19 - 81)	0.391
Total bilirubin (µmol/L)	19.0 (13.8)	19.3 (9.8)	0.956
Creatinine (µmol/L)	161.3 (140.5)	114.4 (31.0)	0.137
Urea (mmol/L)	11.7 (9.0)	9.5 (3.7)	0.349
Mean arterial pressure (mm Hg)	75.3 (11.8)	69.0 (10.8)	0.197
Glasgow Coma Scale score	15 (15 - 15)	15 (15 - 15)	0.436
Days ventilated pre-ECMO	1.5 (1 - 5)	3.5 (0.5 - 6)	0.706
Days on ECMO	9 (2 - 13)	7 (2 - 19)	0.861
Co-infection with bacteria	6 (25.0%)	2 (25.0%)	0.999
CCVH or RRT	19 (79.2%)	8 (100.0%)	0.296

ECMO – extra-corporeal membrane oxygenation; SOFA – sequential organ failure assessment; PEEP – positive end expiratory pressure; H_2O – water; bpm - breaths per minute; $PaO_2/PaCO_2$ – partial pressure of arterial oxygen/carbon dioxide; ALT – alanine aminotransferase; CCVH - continuous venovenous hemofiltration; RRT – renal replacement therapy.

Table 2
Rank correlation coefficient* of clinical characteristics with duration on ECMO.

Variable	N	median (Q1-Q3)	Rank correlation coefficient	p-value
Days on ECMO	32	9 (2 to 14.5)	1	
Body Mass Index	30	29 (26 to 37)	0.094	0.622
SOFA	32	8 (6 to 10.5)	−0.107	0.560
PaO_2:FiO_2 ratio	**32**	**9.3 (7.5 to 11.6)**	**−0.408**	**0.020**
PEEP (cm H_20)	25	12 (12 to 15)	0.047	0.824
Tidal volume (mL)	27	483 (400 to 530)	0.299	0.130
Respiratory rate (bpm)	29	20 (15 to 26)	−0.316	0.095
Peak RR (bpm)	32	30 (27 to 31.5)	0.155	0.396
pH	32	7.26 (7.19 to 7.36)	0.092	0.618
PaO_2 (kPa)	32	7.9 (6.9 to 9.55)	−0.308	0.087
$PaCO_2$ (kPa)	32	7.4 (5.9 to 8.2)	0.032	0.864
Base excess (mmol/L)	32	−1.85 (−5.9 to 2.9)	0.276	0.126
Lactate (mmol/L)	32	1.55 (1.2 to 2.6)	0.055	0.765
Bicarbonate (HCO_3, mmol/L)	32	22.95 (21 to 27.6)	0.065	0.722
C-reactive protein (mg/L)	27	231 (138 to 322)	−0.120	0.552
White cell count (x10^9/L)	32	5.6 (2.6 to 7.9)	−0.065	0.723
Haemoglobin (g/L)	30	125.5 (108 to 148)	0.310	0.095
Platelets (x10^9/L)	32	175.5 (122.5 to 246)	−0.144	0.431
ALT (IU/L)	27	57 (31 to 90)	−0.129	0.522
Total bilirubin (µmol/L)	29	15 (9 to 27)	−0.239	0.212
Creatinine (µmol/L)	32	104 (71 to 194)	−0.205	0.260
Urea (mmol/L)	32	8 (5.1 to 16)	−0.262	0.147
Mean arterial pressure (mm Hg)	32	72 (65 to 82)	−0.121	0.508
Glasgow Coma Scale score	32	15 (15 to 15)	0.295	0.101

ECMO – extra-corporeal membrane oxygenation; SOFA – sequential organ failure assessment; PEEP – positive end expiratory pressure; H_2O – water; bpm - breaths per minute; $PaO_2/PaCO_2$ – partial pressure of arterial oxygen/carbon dioxide; ALT – alanine aminotransferase.

* Rank correlation coefficient measures the strength and direction of a relationship between two variables. The coefficient ranges from −1 to 1 with 1 indicating a strong positive relationship between two variables and −1 indicating a strong negative relationship. A correlation coefficient close to 0 means the relationship between the two variables is very weak.

died (Table 1). However, clinically, these differences are of doubtful significance, as the RR is at the discretion of the parent clinical team prior to referral to ECMO, and the lactate levels are normal in the survivors and only marginally elevated in those who died which will again be dependent on use of CVVH. The higher PaO_2:FiO_2 (P:F) ratio was statistically significantly correlated ($p = 0.020$) with a shorter duration of ECMO, which suggests those with less severe disease recover quicker (Table 2).

Many studies have reported on intensive care patient outcomes of the 2009 influenza A(H1N1)pdm09 pandemic, with or without the use of ECMO. In one study from Australia, where ECMO was used, of 68 patients with confirmed influenza A (53 A(H1N1)pdm09, 8 un-subtyped) infection, 14 (21%) had died mainly due to intracranial and other forms of haemorrhage ($n = 10$), or intractable respiratory failure ($n = 4$).[6] Another study from the USA, where influenza A(H1N1)pdm09-infected patients had non-ECMO ICU admission, of 154 cases, 48 (37%) developed acute respiratory distress syndrome (ARDS), of whom 37 (24%) died.[7] A more recent study from Spain that reviewed influenza A(H1N1)pdm09 cases admitted to ICU (non-ECMO) from 2009–2015, found that of a total of 2421 cases, the mortality ranged from 18.8% (for community-acquired influenza) to 32.9% (for hospital-acquired influenza).[8]

These ECMO-ICU case fatality rates of severe influenza A(H1N1)pdm09 infection are similar to ours of 25% reported here, though compared to the specific ECMO patient cohort,[6] the causes of death in our patients were more variable, including intracranial and other haemorrhage ($n = 3$), sepsis and multi-organ failure ($n = 2$), respiratory failure ($n = 1$), post-cardiopulmonary resuscitation hypoxic brain injury ($n = 1$), and ischaemic bowel associated with atrial fibrillation ($n = 1$).

Thus, even after 10 years of experience with this 'new' pandemic influenza A(H1N1)pdm09 virus, across almost the entire adult age-range (~25–70 years in these previous studies),[6–8] it appears that for severe cases, globally, the survival of such patients appears not to have improved. This may be somewhat surprising as the world's populations have become more immunologically experienced with this virus, which is now considered as a seasonal influenza virus that should be conferring some degree of persisting, cross-reactive individual and herd immunity over consecutive seasons.[9] This may be due to some predisposing genetic or environmental factors in individual patients, which should reinforce the general message that seasonal influenza immunisation is still recommended to minimise the number of people needing ICU or ECMO support for severe influenza infection.

More detailed monitoring on how these physiological parameters change over time (perhaps including more complex cytokine studies), in these severely ill, influenza A(H1N1)pdm09-infected patients admitted to ICU-ECMO units, may eventually yield data to improve their management and clinical outcomes.

Declaration of Competing Interest

None.

References

1. Lam T.T., Tang J.W., Lai F.Y., et al. Comparative global epidemiology of influenza, respiratory syncytial and parainfluenza viruses, 2010-2015. *J Infect* 2019 pii: S0163-4453(19)30218-X[Epub ahead of print]. doi:10.1016/j.jinf.2019.07.008.
2. Tang J.W., Blount J., Bradley C., et al. Impact of a poorly performing point-of-care test during the 2017-2018 influenza season. *J Infect* 2019;**78**(3):249–59. doi:10.1016/j.jinf.2018.10.013.
3. National Health Service (NHS). UK severe flu surveillance system. https://digital.nhs.uk/about-nhs-digital/corporate-information-and-documents/directions-and-data-provision-notices/data-provision-notices-dpns/uk-severe-flu-surveillance-system-data-provision-notice (Accessed 19 Aug 2019).
4. National Health Service (NHS). ICU-HDU influenza surveillance. https://digital.nhs.uk/data-and-information/data-collections-and-data-sets/data-collections/icu-hdu-influenza-surveillance (Accessed 19 Aug 2019).
5. National Health Service England (NHSE) Service specification 170110S. extra corporeal membrane oxygenation (ECMO) for respiratory failure in adults (February 2019). https://www.england.nhs.uk/wp-content/uploads/2019/02/Adult-ECMO-Service-Specification.pdf
6. Davies A., Jones D., et al., Australia and New Zealand Extracorporeal Membrane Oxygenation (ANZ ECMO) Influenza Investigators Extracorporeal membrane oxygenation for 2009 influenza A(H1N1) acute respiratory distress syndrome. *JAMA* 2009;**302**(17):1888–95. doi:10.1001/jama.2009.1535.
7. Bramley A.M., Dasgupta S., Skarbinski J., et al. Intensive care unit patients with 2009 pandemic influenza a (H1N1pdm09) virus infection – United States, 2009. *Influenza Other Respir Viruses* 2012;**6**(6):e134–42.
8. Álvarez-Lerma F., Marín-Corral J., Vilà C., et al. Characteristics of patients with hospital-acquired influenza a (H1N1)pdm09 virus admitted to the intensive care unit. *J Hosp Infect* 2017;**95**(2):200–6. doi:10.1016/j.jhin.2016.12.017.
9. Hancock K., Veguilla V., Lu X., et al. Cross-reactive antibody responses to the 2009 pandemic H1N1 influenza virus. *N Engl J Med* 2009;**361**(20):1945–52. doi:10.1056/NEJMoa0906453.

Matthew Charlton
Anaesthesia and Critical Care, University of Leicester, Leicester, UK
Anaesthesia and Intensive Care, University Hospitals of Leicester, Leicester, UK
Cardiovascular Sciences, University of Leicester, Leicester, UK

Christopher Dunn, Susan Dashey
Anaesthesia and Intensive Care, University Hospitals of Leicester, Leicester, UK

Florence Y. Lai
Cardiovascular Sciences, University of Leicester, Leicester, UK

Julian W. Tang*
Clinical Microbiology, University Hospitals of Leicester, Leicester UK
Respiratory Sciences, University of Leicester, Leicester, UK

*Corresponding author at: Clinical Microbiology, University Hospitals of Leicester, NHS Trust, Level 5 Sandringham Building, Leicester Royal Infirmary, Infirmary Square, Leicester LE1 5WW, UK.
E-mail address: julian.tang@uhl-tr.nhs.uk (J.W. Tang)

Accepted 17 December 2019
Available online 25 December 2019

https://doi.org/10.1016/j.jinf.2019.12.009

Assessment of serum CD5L as a biomarker to distinguish etiology and predict mortality in adults with pneumonia

Dear Editor,

We read with interest the report by Stalenhoef and colleagues in this journal who show that biomarker guided triage can reduce hospitalization rate in community acquired febrile urinary tract infection (REF).[1] Here we report on a prospective observational analysis of the biomarker: CD5 antigen like protein (CD5L), in serum samples collected from 64 patients diagnosed with pneumonia[2] and 44 healthy adults between 2018 and 2019.

The demographic and clinical characteristics of the 64 adults (males 70.3%; mean age 66 ± 20 years) with pneumonia were summarized in Table 1. 57 (89.1%) bacterial pneumonia patients (including 34 patients with confirmed bacterial pneumonia[2] and 23 patients with suspected bacterial pneumonia[3]) and 7(10.9%)

Table 1
Demographic and clinical characteristics of pneumonia and control individuals.

	Bacterial pneumonia				
Characteristics	Total ($n=57$)	SBP ($n=23$)	CBP ($n=34$)	VP ($n=7$)	Healthy controls ($n=44$)
Age (year)	68 ± 19	64 ± 21	71 ± 17	45 ± 10**	53 ± 15
Male sex, *n*(%)	43(75.4%)	17(73.9%)	26(76.5%)	2(28.6%)*	19(43.2%)
WBC (10^9/L)	15 ± 8	14 ± 9	16 ± 8	8 ± 5*	6 ± 1
NEU%	85 ± 10	84 ± 10	86 ± 9	70 ± 15**	56 ± 8
CRP (mg/L)	76(59,90)	76(58,76)	79(58,90)	34(8,45)*	NA
PCT (ng/mL)	0.71(0.22,7.07)	0.43(0.10,6.14)	1.03(0.37,8.07)	0.07(0.05,0.14)**	NA
CD5L (ng/ml)	618 ± 279	557 ± 264	659 ± 284	275 ± 148**	116 ± 45
APACHE II	16 ± 6	13 ± 5	18 ± 6	10 ± 5*	NA
SOFA	5 ± 3	4 ± 3	5 ± 4	3 ± 2	NA
ICU stay (days)	11(5,18)	6(3,13)	14(6,20)	0(0,4)**	NA
Nonsuvivors, *n*(%)	17(29.8%)	6(26.1%)	11(32.4%)	1(14.3%)	NA
Hypertension, *n*(%)	25(43.9%)	7(30.4%)	18(52.9%)	1(14.3%)	NA
Diabetes, *n*(%)	16(28.1%)	6(26.1%)	10(29.4%)	1(14.3%)	NA
CRF, *n*(%)	9(15.8%)	4(17.4%)	5(14.7%)	0	NA
Hepatic dysfunction, *n*(%)	2(3.5%)	1(4.3%)	1(2.9%)	1(14.3%)	NA
Cerebrovascular disease, *n*(%)	4(12.9%)	0	4(11.8%)	0	NA
Surgery within 3 months, *n*(%)	1(3.2%)	0	1(2.9%)	0	NA
CHF, *n*(%)	10(17.5%)	4(17.4%)	6(17.6%)	0	NA
CRI, *n*(%)	13(22.8%)	3(13%)	10(29.4%)	0	NA
Pneumonia type (CAP/HAP)	17,107	21/2	25/9	7/0	NA

NOTE. Data normally distributed were reported as means±SD, non-normally distributed were reported as medians (IQR).
SBP: suspected bacterial pneumonia; CBP: confirmed bacterial pneumonia; VP: viral pneumonia; WBC: white blood cell; NEU%: neutrophil percentage; CRP: C-reaction protein; PCT: procalcitonin; CD5L: CD5 antigen like protein; APACHE II: acute physiology and chronic health evaluation II; SOFA: sequential organ failure assessment; ICU: intensive care unit; CRF: chronic renal failure; CHF: chronic heart failure; CRI: chronic respiratory insufficiency; CAP: community-acquired pneumonia; HAP: hospital-acquired pneumonia; NA: not applicable.
*$p < 0.05$ when compared with total bacterial pneumonia (Mann–Whitney *U* test or Student *T* test).
**$p < 0.01$ when compared with total bacterial pneumonia (Mann–Whitney *U* test or Student *T* test).
***$p < 0.001$ when compared with total bacterial pneumonia (Mann–Whitney *U* test or Student *T* test).

viral pneumonia patients were studied. There were significant differences in age, sex, WBC, NEU%, CRP, PCT, CD5L, APACHE II scores and length of ICU stay between bacterial pneumonia and viral pneumonia. The pathogens responsible for pneumonia were described in Supplementary Table 1. Globally, Gram-negative bacteria infection is more common than Gram-positive bacteria infection in pneumonia. Among them, *Acinetobacter baumannii* (16, 59.3%) was considered the major pathogen in gram-negative bacteria and *Staphylococcus aureus* (3, 42.9%) was considered the major pathogen in Gram-positive bacteria. In viral pneumonia, influenza A (H1N1) was detected as the unique pathogen.

In the study of the diagnostic performance of serum CD5L to identify etiology of pneumonia, as we found in Supplementary Fig. 1, no matter in total bacterial pneumonia, suspected bacterial pneumonia or confirmed bacterial pneumonia, the serum of CD5L levels on day of pneumonia diagnosis were significantly higher than those in viral pneumonia and healthy control subjects. For evaluating the diagnostic performance of CD5L to differentiate bacterial from viral infection in pneumonia, ROC analysis was conducted for the above bacterial pneumonia (Supplementary Fig. 2) and compared with routine laboratory markers (Table 2). By horizontal comparison, we found that the best AUC was for CD5L (AUC=0.89), better than NEU% (AUC = 0.79), WBC (AUC = 0.79), CRP (AUC = 0.78) and even PCT (AUC = 0.85). Interestingly, by longitudinal comparison, the AUC was observed highest in confirmed bacterial pneumonia (AUC = 0.92), intermediate in all bacterial pneumonia (AUC = 0.89), and lowest in suspected bacterial pneumonia (AUC = 0.84), which may better elucidate the diagnostic performance of CD5L for etiology diagnosis in pneumonia patients. Although there are 23 patients with suspected bacterial pneumonia for which no definitive pathogen was found, our result here may still provide a new treatment for bacterial infection identification in pneumonia patients for the current limitations in direct pathogen testing make it difficult to identify the pathogen at the time of diagnosis[4]. Besides, as a potential biomarker to distinguish pathogens[5–8], CD5L levels were also significantly correlated with WBC, NEU%, CRP and PCT (Supplementary Fig. 3) in patients with pneumonia.

In the study of the diagnostic performance of serum CD5L to predict mortality in adults with pneumonia, mortality was defined as death occurring within 30 days after the onset of pneumonia. As we observed in Supplementary Fig. 4A, serum CD5L levels on day of pneumonia diagnosis were significantly higher in non-survivors ($n = 18$) than survivors ($n = 46$) ($p < 0.001$). To ensure that serum CD5L levels were not influenced by the class of the infection in the specimens, Spearman's rank correlation analysis was performed between serum CD5L levels and poor prognosis related scores[9,10] (SOFA and APACHE II scores) in patients with total bacterial pneumonia, suspected bacterial pneumonia, confirmed bacterial pneumonia and viral pneumonia, respectively. Our correlation analysis between serum CD5L levels and SOFA or APACHE II scores shows that no matter for bacterial pneumonia or viral pneumonia, the CD5L levels showed positive correlation with SOFA and APACHE II scores (Supplementary Figs. 5 and 6). Furthermore, the AUC of CD5L for identifying 30-day mortality in adult pneumonia patients was 0.79 (Supplementary Fig. 4B), a value means good diagnostic performance, which is consistent with Gao's study[9] before.

Therefore, we found that determining serum CD5L concentrations on day of pneumonia diagnosis was of great value in identifying bacterial infection from viral infection and predicting 30-day mortality in adult patients with pneumonia, which suggests that CD5L may work for the etiologic diagnosis and could represent a novel biomarker for identification of a group of patients with pneumonia presenting with higher risk of death. These findings encourage further efforts aimed at exploring the clinical value of circulating CD5L to help early clinical decision-making in human pneumonia.

Table 2
AUC and optimal cut-off points with their corresponding validity indexes and predictive values for differentiating bacterial from viral infection in adult patients with pneumonia.

	Cut-off value	AUC (95%CI)	Se (%)	Sp (%)	J (%)	PPV (%)	NPV (%)
Total BP							
CD5L (ng/mL)	336.52	0.89(0.79–0.95)	85.7	93.0	78.70	98.1	60.0
NEU% (%)	76.5	0.79(0.67–0.88)	85.7	84.2	69.92	98.0	40.0
WBC (10^9/L)	9.51	0.79(0.68–0.89)	85.7	71.9	57.62	97.6	27.3
CRP (mg/L)	44.9	0.78(0.66–0.87)	85.7	78.9	64.66	97.8	33.3
PCT (ng/mL)	0.14	0.85(0.74–0.93)	85.7	84.2	69.92	98.0	40.0
Suspective BP							
CD5L (ng/mL)	336.52	0.84(0.66–0.95)	85.7	87.0	72.67	66.7	95.2
NEU% (%)	76.5	0.78(0.59–0.91)	85.7	82.6	68.32	60.0	95.0
WBC (10^9/L)	6.93	0.78(0.60–0.91)	71.4	87.0	58.39	62.5	90.9
CRP (mg/L)	44.9	0.76(0.57–0.90)	85.7	78.3	63.98	54.5	94.7
PCT (ng/mL)	0.14	0.79(0.60–0.91)	85.7	69.6	55.28	46.2	94.1
Confirmed BP							
CD5L (ng/mL)	336.52	0.92(0.79–0.98)	85.7	97.1	82.77	85.7	97.1
NEU% (%)	76.5	0.79(0.64–0.90)	85.7	85.3	71.01	54.5	96.7
WBC (10^9/L)	9.51	0.80(0.65–0.91)	85.7	79.4	65.13	46.2	96.4
CRP (mg/L)	44.9	0.79(0.64–0.90)	85.7	79.4	65.13	46.2	96.4
PCT (ng/mL)	0.14	0.89(0.75–0.97)	85.7	94.1	79.83	75.0	97.0

CD5L: CD5 antigen like protein; NEU%: neutrophil percentage; WBC: white blood cell; CRP: C-reaction protein; PCT: procalcitonin; 95%CI: 95% confidence interval; Se: sensitivity; Sp: specificity; J: Youden index; PPV: positive predictive value; NPV: negative predictive value; BP: bacterial pneumonia.

Declaration of Competing Interest

None.

Acknowledgments

We would like to thank the patients and healthy volunteers in The First Affiliated Hospital of Chongqing Medical University for their cooperation and support. This work has been financially supported by National Natural Science Foundation of China (No. 81902134 and No. 81722001).

Supplementary materials

Supplementary material associated with this article can be found, in the online version, at doi:10.1016/j.jinf.2019.12.003.

References

1. Stalenhoef J.E., van Nieuwkoop C., Wilson D.C., van der Starre W.E., Delfos N.M., Leyten E.M.S., et al. Biomarker guided triage can reduce hospitalization rate in community acquired febrile urinary tract infection. *J Infect* 2018;**77**(1):18–24.
2. Niederman M.S., Mandell L.A., Anzueto A., Bass J.B., Broughton W.A., Campbell G.D., et al. Guidelines for the management of adults with community-acquired pneumonia. Diagnosis, assessment of severity, antimicrobial therapy, and prevention. *Am J Respir Crit Care Med* 2001;**163**(7):1730–54.
3. Haran J.P., Buglione-Corbett R., Lu S.. Cytokine markers as predictors of type of respiratory infection in patients during the influenza season. *Am J Emerg Med* 2013;**31**(5):816–21.
4. Self W.H., Wunderink R.G., Jain S., Edwards K.M., Grijalva C.G.. Procalcitonin as a marker of etiology in adults hospitalized with community-acquired pneumonia. *Clin Infect Dis Off Publ Infect Dis Soc Am* 2018;**66**(10):1640–1.
5. Gao X., Yan X., Zhang Q., Yin Y., Cao J.. CD5L contributes to the pathogenesis of methicillin-resistant Staphylococcus aureus-induced pneumonia. *Int Immunopharmacol* 2019;**72**:40–7.
6. Kimura H., Suzuki M., Konno S., Shindou H., Shimizu T., Nagase T., et al. Orchestrating role of apoptosis inhibitor of macrophage in the resolution of acute lung injury. *J Immunol* 2017;**199**(11):3870–82 (Baltimore, Md: 1950).
7. Kuwata K., Watanabe H., Jiang S.Y., Yamamoto T., Tomiyama-Miyaji C., Abo T., et al. AIM inhibits apoptosis of T cells and NKT cells in corynebacterium-induced granuloma formation in mice. *Am J Pathol* 2003;**162**(3):837–47.
8. Martinez V.G., Escoda-Ferran C., Tadeu Simoes I., Arai S., Orta Mascaro M., Carreras E., et al. The macrophage soluble receptor AIM/Api6/CD5L displays a broad pathogen recognition spectrum and is involved in early response to microbial aggression. *Cell Mol Immunol* 2014;**11**(4):343–54.
9. Gao X., Liu Y., Xu F., Lin S., Song Z., Duan J., et al. Assessment of apoptosis inhibitor of macrophage/CD5L as a biomarker to predict mortality in the critically ill with sepsis. *Chest* 2019;**156**(4):696–705.
10. Kao S.J., Yang H.W., Tsao S.M., Cheng C.W., Bien M.Y., Yu M.C., et al. Plasma long pentraxin 3 (PTX3) concentration is a novel marker of disease activity in patients with community-acquired pneumonia. *Clin Chem Lab Med* 2013;**51**(4):907–13.

Tangtian Chen[1]
Department of Laboratory Medicine, The First Affiliated Hospital of Chongqing Medical University, No.1 Friendship Road, Yuzhong District, Chongqing 400016, China

Jun Duan[1]
Department of Respiratory and Critical Care Medicine, The First Affiliated Hospital of Chongqing Medical University, Chongqing 400016, China

Mengmeng Li, Xianan Wu, Ju Cao*
Department of Laboratory Medicine, The First Affiliated Hospital of Chongqing Medical University, No.1 Friendship Road, Yuzhong District, Chongqing 400016, China

*Corresponding author.
E-mail address: caoju723@163.com (J. Cao)

[1] These authors contributed equally to this work.
Accepted 6 December 2019
Available online 16 December 2019

https://doi.org/10.1016/j.jinf.2019.12.003

Two newly identified genotypes for African swine fever virus are incorrect

Dear editor,

Recently, a study in this journal identified two novel genotypes (XXV and XXVI) for African swine fever viruses (ASFVs).[1] ASF is a severe viral disease affecting domestic and wild pigs and shows

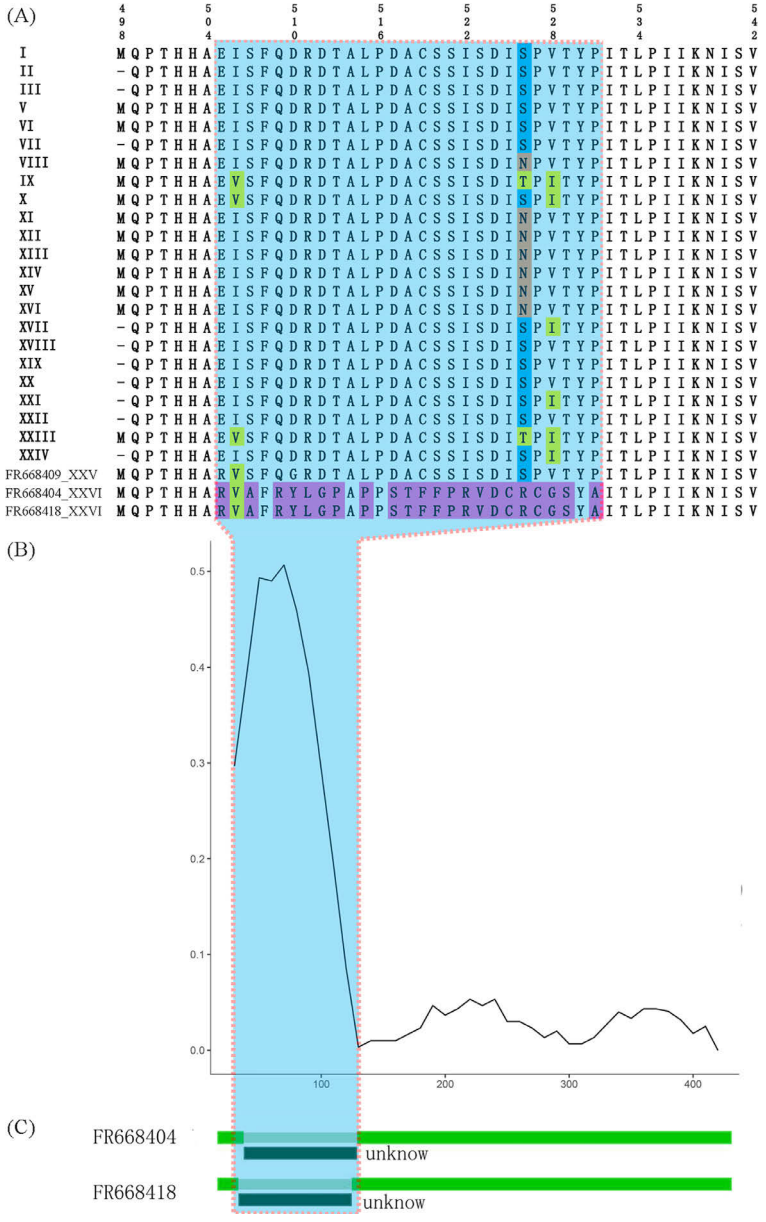

Fig. 1. Analysis of p72 genotypes. (A) p72 amino acid sequences from genotypes XXV (FR668409) and XXVI (FR668404 and FR668418) compared to the other 24 genotypes. (B) Sliding window genetic distances between genotype XXVI and the other 24 genotypes from 60 bp long sliding windows, with step size of 10 bp, across the p72 sequence. (C) Analysis for recombination shows that the two genotype XXVI sequences have a region of non-homology.

high morbidity and mortality (up to 100%). ASF is a devastating threat to pig agriculture and is responsible for serious production and economic losses. The ASFV genome is 170–193 kilo base pairs in length [2] and has been divided into 24 different genotypes based on their B646L gene sequence, a gene which encodes the capsid protein p72.[3,4]

Our previous study showed that the p72 gene located in a very low genetic diversity region of the genome.[5] Ye and colleagues, however, identified two novel genotypes XXV and XXVI, with genotype XXVI being especially divergent from all other genotypes.[1] To examine this unexpected result, in this study, we reanalyzed their data to evaluate the reliability of these two genotypes. We collected 716 available p72 gene sequences from NCBI (http://www.ncbi.nlm.nih.gov/), which we then aligned with MAFFT software, a fast multiple sequence alignment program.[6] The alignments show that genotype XXV (accession number FR668409) has a single amino acid change at position 506 compared to genotype I, while for genotype XXVI (accession numbers FR668404 and FR668418), the region coding for amino acid residues 509 to 528 differs greatly compared to all other genotypes (Fig. 1A). To examine this in greater detail, we calculated genetic distance across the p72 coding sequence in 60 bp sliding windows, with a step size of 10 bp, between these two sequences and the 24 other genotypes (Fig. 1B). This sliding window analysis shows these two sequences for genotype XXVI have a region that is very divergent, with genetic distance up to 0.5067 from the other genotypes,

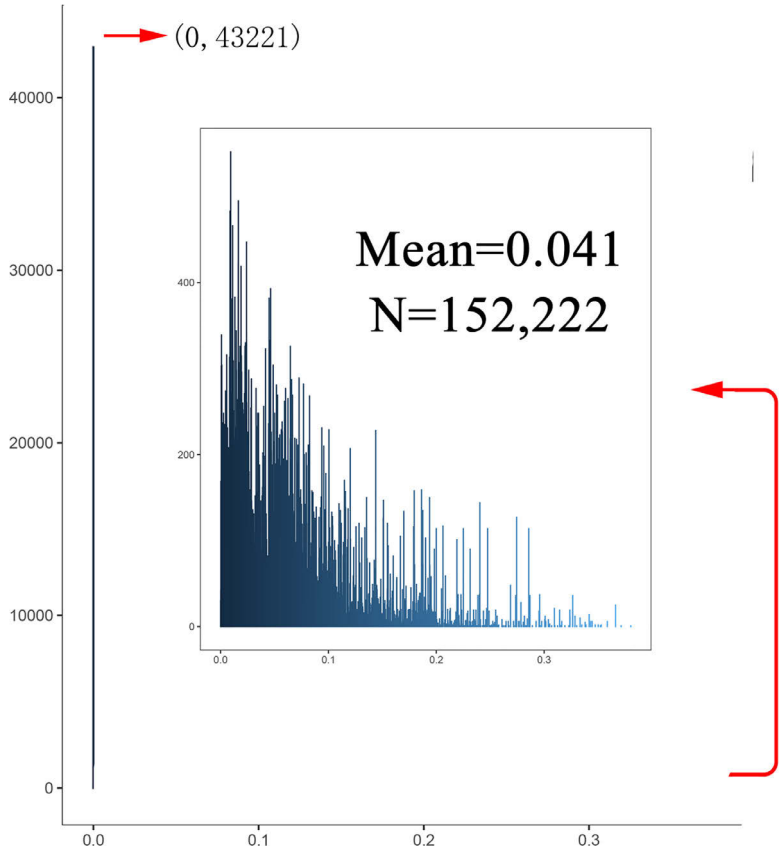

Fig. 2. Distribution of pairwise genetics distances between genes of different genotypes in ASFVs. Coding sequences for 182 ASFV genes of ASFVs were extracted from 42 available ASFV genomes. Pairwise genetic distances of each pair of genes was calculated and plotted.

while the genetic distances of the remaining regions are less than 0.1 (Fig. 1B).

Genetic distances for ASFVs were calculated for 182 coding gene sequences, from 42 available complete genomes of ASFVs, to assess the overall divergence. Pairwise genetic distances of each gene for all ASFV strains were calculated. The mean pairwise genetic distance for ASFV genes was 0.041 (Fig. 2), which is much lower than this divergent region of these two sequences for genotype XXVI (0.5067). Therefore, it seems highly unlikely that a gene has such a highly divergent region.

Since recombination frequently occurs in ASFVs,[5] we conducted a recombination analysis with the RDP4 program, which used the 3seq, bootscan, chimaera, genecov, lard, maxchi, rdp and siscan detection methods,[7] to determine whether recombination might have occurred in the XXVI genotype. We found reliable evidence for recombination events in both p72 genotype XXVI sequences (Fig. 1C). This suggests that the very highly divergent region of this p72 genotype is not homologous with other p72 genotypes. We used Blastn, from NCBI (https://blast.ncbi.nlm.nih.gov/Blast.cgi), to identify a source for this highly divergent region, however, no similarity sequence was found.

We then mapped the multiple amino acid changes found in genotype XXVI to the 3D structure of p72 (Fig. 3). The changed sites (marked in red in Fig. 3) are located in the Dec loop, a region which plays an important role in the formation of the trimer spike.[8] The amino acid mutations result in changes of electrostatic potential, hydrophobicity, and steric hindrance. It seems unlikely to have so many changes in such a functionally important region.

In our previous studies we noticed that sequences directly submitted by individual laboratories to GenBank often contain errors such as misidentification of species, sampling error, contamination, or are pseudogenes, which can lead to sequence analysis problems and erroneous conclusions.[9,10] Sequences that deviate from the overall intraspecific pairwise divergence are potentially erroneous.[9,10] Since genotype XXVI deviates from other genotypes not only in genetic distance, but also in protein structure, and mutations occur in the flanking regions of the sequences, we deduced that these reported mutations might be due to low quality sequencing. We identified the original manuscript reporting the three sequences of genotypes XXV and XXVI,[11] where the authors stated that the “Alignment and translation of sequences obtained from Sardinian isolates revealed that the C-terminal end of p72 gene was completely conserved between the sequences compared”. This statement indicates that these sequences did not considerably diverge from previously reported ASFV p72 sequences, and thus, suggests that an error in these sequences had been introduced upon submitting them to GenBank. Further examination of the original samples and sequences is needed. We contacted the corresponding author of this manuscript to check these three sequences, and were told that these three p72 sequences were all genotype I, and had some errors when submitted to GenBank.

In conclusion, the two novel genotypes of ASFVs (XXV and XXVI) identified by Ye and colleagues [1] are misled by problematic sequences. As reminded by our previous studies, many problematic sequences are present in GenBank, which can lead to problems in downstream analyses.[9,10] Thus, when published data is used for new analyses, the first set in the process of data analyses should

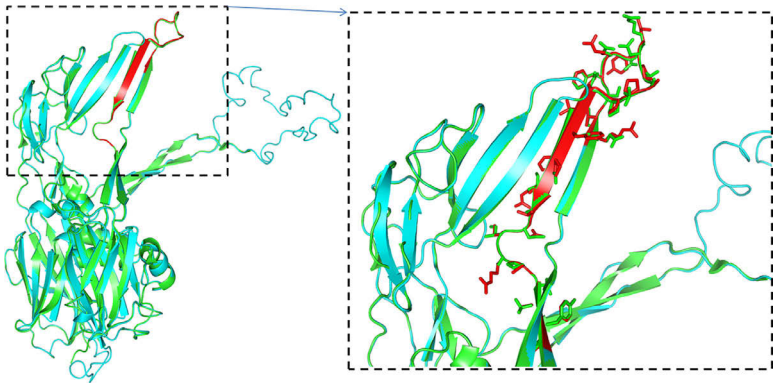

Fig. 3. Locations of amino acid sites with changes in genotype XXVI mapped to the 3-dimensional structure of p72. These amino acid changes marked in red are located in the Dec loop.

be to filter these sequences for potential errors to reduce the possibility of reaching incorrect conclusions. If conclusions are based on obviously strange sequences, then we should trace back the data to their original source, and manuscript, and contact the corresponding authors before making conclusions based on these sequences.

Declaration of Competing Interest

The authors declare no conflict of interest.

Acknowledgments

This work was supported by the National Natural Science Foundation of China (No. 31822056), Key Program of Department of Education of Guangdong Province, Key Realm R&D Program of Guangdong Province (No. 2019B020211004), the 111 Project and the third batch of Zhaoqing Xijiang innovation team project.

References

1. Ye C., Wu X., Chen T., Huang Q., Fang R., An T.. The updated analysis of African swine fever virus genomes: two novel genotypes are identified. *J Infect* 2019. doi:10.1016/j.jinf.2019.10.013.
2. Dixon L.K., Chapman D.A., Netherton C.L., Upton C.. African swine fever virus replication and genomics. *Virus Res* 2013;**173**(1):3–14.
3. Shen X., Pu Z., Li Y., Yu S., Guo F., Luo T., et al. Phylogeographic patterns of the African swine fever virus. *J Infect* 2019;**79**(2):174–87.
4. Quembo C.J., Jori F., Vosloo W., Heath L.. Genetic characterization of African swine fever virus isolates from soft ticks at the wildlife/domestic interface in Mozambique and identification of a novel genotype. *Transbound Emerg Dis* 2018;**65**(2):420–31.
5. Li X., Xiao K., Zhang Z., Yang J., Wang R., Shen X., et al. The recombination hot spots and genetic diversity of the genomes of African swine fever viruses. *J Infect* 2019. doi:10.1016/j.jinf.2019.08.007.
6. Katoh K., Toh H.. Parallelization of the MAFFT multiple sequence alignment program. *Bioinformatics* 2010;**26**(15):1899–900.
7. Martin D.P., Murrell B., Golden M., Khoosal A., Muhire B.. RDP4: detection and analysis of recombination patterns in virus genomes. *Virus Evol* 2015;**1**(1):vev003.
8. Liu Q., Ma B., Qian N., Zhang F., Tan X., Lei J., et al. Structure of the African swine fever virus major capsid protein p72. *Cell Res* 2019;**29**(11):953–5.
9. Li X., Shen X., Chen X., Xiang D., Murphy R.W., Shen Y.. Detection of potential problematic CYTB gene sequences of fishes in Genbank. *Front Genet* 2018;**9**:30.
10. Shen Y., Chen X., Murphy R.W.. Assessing DNA barcoding as a tool for species identification and data quality control. *PLoS One* 2013;**8**(2):e57125.
11. Giammarioli M., Gallardo C., Oggiano A., Iscaro C., Nieto R., Pellegrini C., et al. Genetic characterisation of African swine fever viruses from recent and historical outbreaks in Sardinia (1978–2009). *Virus Genes* 2011;**42**(3):377–87.

Xianghui Liang[1]
College of Veterinary Medicine, South China Agricultural University, Guangzhou 510642, China

Rui Li[1]
Key Laboratory of Animal Immunology of the Ministry of Agriculture, Henan Provincial Key Laboratory of Animal Immunology, Henan Academy of Agricultural Sciences, Zhengzhou 450002, China

Xuejuan Shen, Kangpeng Xiao, Xiaobing Li
College of Veterinary Medicine, South China Agricultural University, Guangzhou 510642, China

David M. Irwin
Department of Laboratory Medicine and Pathobiology, University of Toronto, Toronto, M5S 1A8, Canada
Banting and Best Diabetes Centre, University of Toronto, Toronto, M5S 1A8, Canada

Yongyi Shen*
College of Veterinary Medicine, South China Agricultural University, Guangzhou 510642, China
Zhaoqing Institute of Biotechnology, Zhaoqing 526238, China

*Corresponding author at: College of Veterinary Medicine, South China Agricultural University, Guangzhou 510642, China.
E-mail address: shenyy@scau.edu.cn (Y. Shen)

[1] Both authors contributed equally to this work.
Accepted 26 November 2019
Available online 30 November 2019

https://doi.org/10.1016/j.jinf.2019.11.020

Identification of a new HCV subtype 6xi among chronic hepatitis C patients in Yunnan, China

Dear Editor,

Recent correspondence in this Journal has highlighted that accurate determination of Hepatitis C Virus (HCV) genotype/subtype can be critical; as this may impact response to direct-acting antiviral (DAA) therapies.[1] Chronic HCV infection is a major cause of cirrhosis and hepatocellular carcinoma. It was reported that approximate 71 million people worldwide had chronic HCV infection with about 1.75 million new HCV infections and about

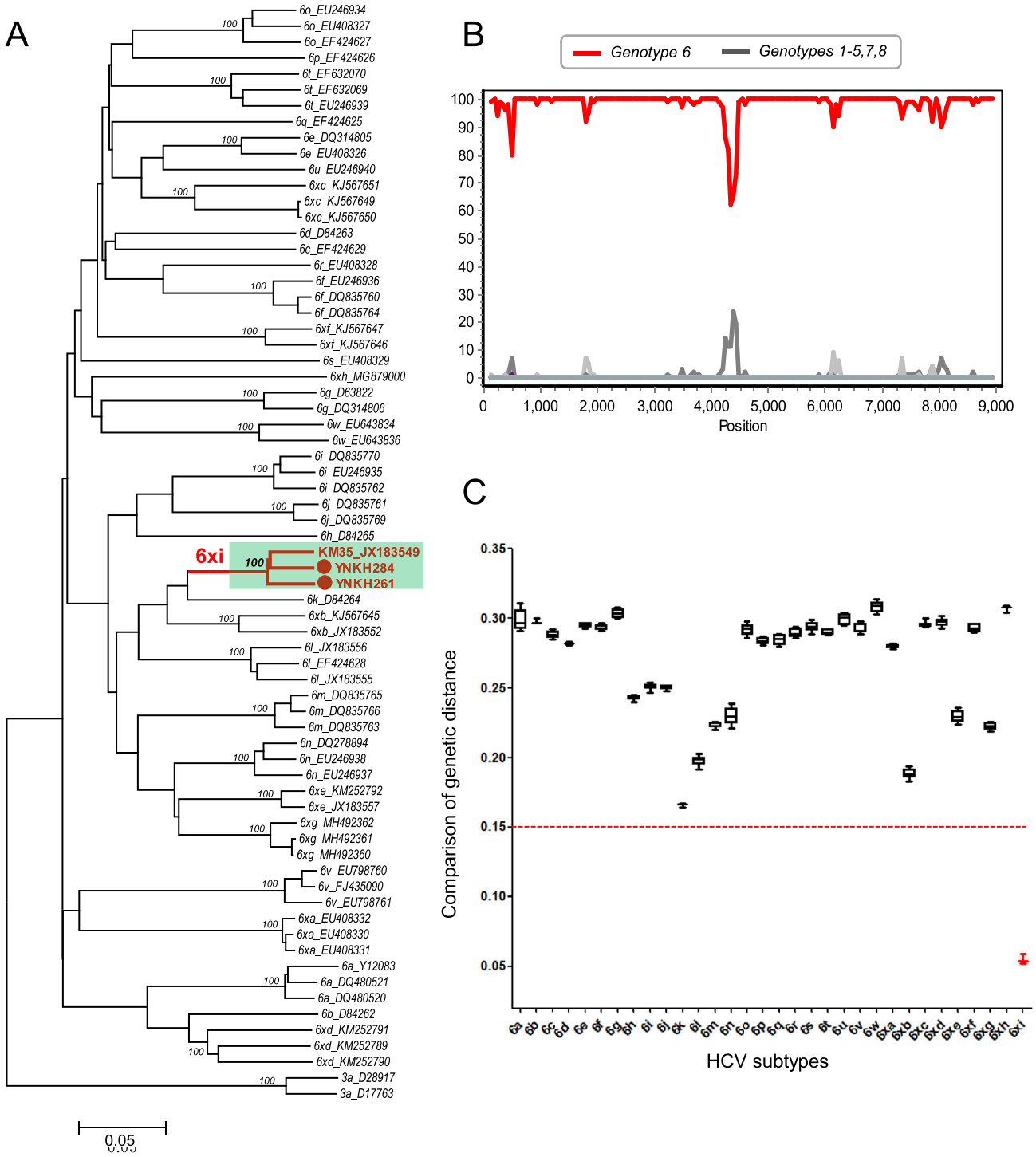

Fig. 1. The analyses of phylogenetic tree, recombinant, and nucleotide divergence between 6xi and the other known 6 subtypes (6a–6xh) based on full-length HBV genome sequences. (A) The known HCV subtype 6 reference sequences (6a–6xh) from the previous report were used. Phylogenetic analysis was performed by the maximum-likelihood method, based on the GTR +G+I substitution model, with 1000 bootstrap replicates using the software MEGA v6. The sequences of HCV 6xi (YNKH261 and YNKH284) are marked in red dot. (B) Bootscan plots were constructed using Simplot 3.5.1 software based on 100 replicates with a 300-bp sliding window moving in steps of 50 bases. (C) Pairwise comparisons of nucleotides similarities between 3 HCV 6xi strains and 30 reference genotype 6 sequences.

399,000 deaths per year.[2] Currently, DAA treatment regimens that target NS3/NS4A protease, NS5A phosphor-protein and the NS5B polymerase have shown high safe and high rates of sustained virologic response in HCV chronically infected patients (>90%).[3] However, under selective pressure from these drugs, drug resistance-associated substitutions (RAS) can emerge during this therapy and result in treatment failure in 2−10% of patients.[4] Therefore, HCV infection is still a major global health concern.

To date, eight confirmed genotypes have been characterized based on >30% sequence divergence in the complete HCV genome, and genotypes are further classified into >80 subtypes with a sequence divergence of >15% to other subtypes of the same geno-

type.[5] In the current study, we characterized a new HCV subtypes among chronic hepatitis C patients in Yunnan, China, initially designated as 6xi, further analyzed its evolutionary history and investigated its baseline RAS by next generation sequencing (NGS) method.

Plasma samples were collected between January 2018 and October 2018 from 160 chronic hepatitis C patients from Kunming city in Yunnan, China (Fig. S1A). The samples met the following inclusion criteria: (1) hepatitis C antibody-positive for 6 months with normal serum alanine aminotransferase (ALT) levels; (2) subject was residing in Yunnan province and was over 18 years old; (3) complete demographic information and clinical data were available; (4) consented to the use of patient information in studies on HCV epidemics; and (5) were treatment-naïve during sampling. There was no epidemiologic link among these individuals. The study was approved by the First People's Hospital of Yunnan Province Ethics Committee. Written informed consent was obtained from all participants prior to the study.

Out of a total of 160 chronic hepatitis C patients, 152 partial NS5B gene fragments were successfully amplified and sequenced with a success rate of 95.0% (152/160). Multiple subtypes were identified in 152 subjects, including subtype 3b (36.2%, 55/152), 3a (23.7%, 36/152), 1b (19.1%, 29/152), 2a (8.5%, 13/152), 6n (7.9%, 12/152), 6a (2.0%, 3/152), and 1a (1.3%, 2/152) (Fig. S1B). Interestingly, the remaining two strains (1.3%, 2/152) involving YNKH261 and YNKH284 together with the isolate KM35 reported formed a novel separate cluster in the genotype 6 with an 82% bootstrap value, indicating a potential new HCV subtype 6.

To confirm that the two strains belong to a novel HCV subtype 6, their complete genome sequences were successfully amplified and sequenced with 12 overlapping fragments. Further, phylogenetic analysis was performed along with HCV reference sequences of representative subtypes 6a–6xh. The result showed that the two strains and isolate KM35 formed a distinct monophyletic cluster supported by a high bootstrap value of 100%. The three strains were isolated from three HIV-1 infected patients without obvious epidemiological linkage in Yunnan and showed no evidence of recombination using Bootscan analysis (Fig. 1(B)). Moreover, the intergroup nucleotide divergence (mean ± SD) % over the full-length genome sequences of the isolates (YNKH261, YNKH284, and KM35) were compared to that of representative subtypes (6a–6xh) (Fig. 1(C)). The results revealed that the three strains were different from known HCV subtypes of 6a–6xh by 16.5–28.5%. Therefore, the three strains are initially designated 6xi.

To better understand the time of emergence of HCV 6xi, we performed bayesian molecular clock analyses using full-length genome sequences to estimate the time to the most recent common ancestor (tMRCA). As shown in Fig. 2(A), the estimated tMRCAs for the genotype 6xi was 1971.1 [95% highest probability density (HPD): 1951.1, 1991.4]. In addition, to further investigate baseline RAS of subtype 6xi, naturally occurring resistance-associated substitutions (RAS) were analyzed for the NS3, NS5A and NS5B sequences using next generation sequencing (NGS) method. Strikingly, HCV 6xi strains contain the substitution 28 V with a 100% frequency of mutations in the NS5A protein contributing to resistance to Velpatasvir of NS5A phosphoprotein inhibitor,[6] suggesting that the subtype 6xi maybe basically resistant to NS5A inhibitors (Fig. 2(B)).

Among the HCV eight genotypes, genotype 6 exhibits a high degree of genetic complexity and diversity, and 31 subtypes have been confirmed by the International Committee on Taxonomy of Viruses.[7] In China, HCV genotype 6 is common, and subtype 6a is the most prevalent subtype, primarily distributed in Guangdong, 6n is the second most prevalent subtype, mainly found in Yunnan, followed by subtypes 6xa, 6 g, 6v, 6 w, 6e, 6b, 6j, 6q,and 6r among genotype 6 isolates.[8–10] To our knowledge, 6xi is the eighth detection of novel HCV subtypes 6 in China combined with previously identified 6a, 6e, 6n, 6v, 6xa, 6xe and 6xh, resulting in genotype 6 to expand to 32 subtypes in the world. Our findings again demonstrated that HCV genotype 6 was more complex and diverse.

In summary, we characterized a new HCV subtype 6xi based on the characteristics of a monophyletic cluster, > 15% genetic distances, no significant evidence of recombination, and no epidemiologic link among individuals. In addition, bayesian analyses showed that 6xi may originate around the year 1971, and the strains of HCV

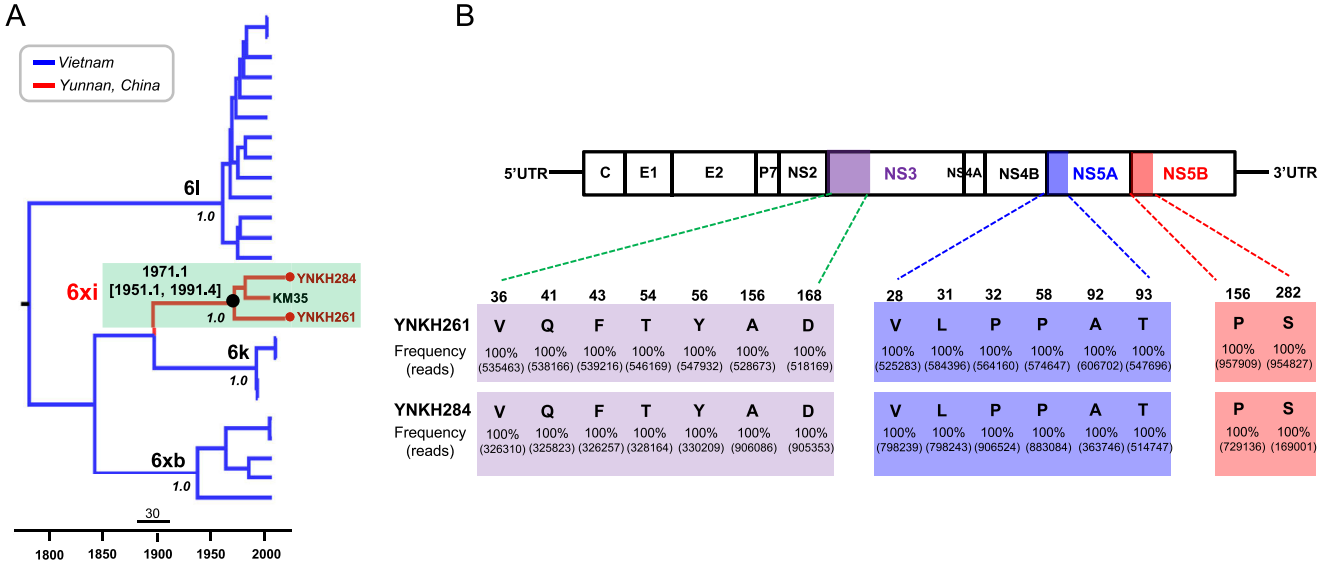

Fig. 2. The maximum clade credibility (MCC) trees of HCV full-length genome sequences and the analyses of DAA resistance-associated substitutions. (A) The MCC tree was constructed by Bayesian MCMC analysis based on the uncorrelated log-normal relaxed clock model with the GTR+I+G nucleotide substitution mode using BEAST software. The numbers on the branches represent the posterior probability values. Timescale is shown at the bottom of the tree. The mean the most recent common ancestor (tMRCA) and 95% highest probability density (HPD) for the key nodes are indicated. HCV 6xi strains from Yunnan are highlighted in red. (B) Naturally occurring resistance-associated substitutions (RAS) were analyzed for the NS3, NS5A and NS5B sequences by next generation sequencing (NGS) method. The potential direct-acting antivirals resistance-associated substitutions of HCV subtype 6 are from the latest report in 2018.[6]

6xi naturally contain the substitution 28 V in the NS5A protein contributing to resistance to Velpatasvir of NS5A phosphoprotein inhibitor. The present finding again highlights the genetic characteristics and HCV strains in Yunnan, and the urgent need for continuous molecular screening and epidemic surveillance in Yunnan to implement effective measures to reduce HCV transmission.

Declaration of Competing Interest

The authors declare no competing financial interests.

Acknowledgments

We thank the members of the clinical laboratory in the First People's Hospital of Yunnan Province for the clinical data and sample collection.

Funding

This work was supported by the Major special projects and key R & D projects in Yunnan Province (2019ZF004), the Key projects of Yunnan applied basic research plan (2019FA005), the Reserve Talents Project for Young and Middle-Aged Academic and Technical Leaders of Yunnan Province (2019HB012), the Science and Technology Department of Yunnan Province (2018DG010), Youth Talent Program of Yunnan "Ten-thousand Talents Program" (YNWR-QNBJ-2018-054), and the Medical Leading Talent Program of Yunnan Province (L-201618).

Supplementary materials

Supplementary material associated with this article can be found, in the online version, at doi:10.1016/j.jinf.2019.11.019.

References

1. Bradshaw D., Mbisa J.L., Geretti A.M., Healy B.J., Cooke G.S., Foster G.R., et al. Consensus recommendations for resistance testing in the management of chronic hepatitis c virus infection: Public Health England HCV Resistance Group. *J Infect* 2019;**S0163-4453**(19) 30317-2.
2. Indolfi G., Easterbrook P., Dusheiko G., El-Sayed M.H., Jonas M.M., Thorne C., et al. Hepatitis C virus infection in children and adolescents. *Lancet Gastroenterol Hepatol* 2019;**4**(6):477–87.
3. Vermehren J., Park J.S., Jacobson I.M., Zeuzem S.. Challenges and perspectives of direct antivirals for the treatment of hepatitis C virus infection. *J Hepatol* 2018;**69**(5):1178–87.
4. von Massow G., Garcia-Cehic D., Gregori J., Rodriguez-Frias F., Macià M.D., Escarda A., et al. Whole-genome characterization and resistance-associated substitutions in a new HCV genotype 1 subtype. *Infect Drug Resist* 2019;**12**:947–55.
5. Hedskog C., Parhy B., Chang S., Zeuzem S., Moreno C., Shafran S.D., et al. Identification of 19 novel hepatitis C virus subtypes-further expanding HCV classification. *Open Forum Infect Dis* 2019;**6**(3):ofz076.
6. Sorbo M.C., Cento V., Di Maio V.C., Howe A.Y.M., Garcia F., Perno C.F., et al. Hepatitis C virus drug resistance associated substitutions and their clinical relevance: update 2018. *Drug Resist Updat* 2018;**37**:17–39.
7. Ye M., Chen X., Wang Y., Duo L., Zhang C., Zheng Y.T.. Identification of a new HCV subtype 6xg among injection drug users in Kachin, Myanmar. *Front Microbiol* 2019;**10**:814.
8. Chen Y., Yu C., Yin X., Guo X., Wu S., Hou J.. Hepatitis C virus genotypes and subtypes circulating in Mainland China. *Emerg Microbes Infect* 2017;**6**(11):e95.
9. https://talk.ictvonline.org/ictv_wikis/flaviviridae/w/sg_flavi/634/table-1-confirmed-hcv-genotypes-subtypes-may-2019. 2019.
10. Huang K., Chen J., Xu R., Jiang X., Ma X., Jia M., et al. Molecular evolution of hepatitis C virus in China: a nationwide study. *Virology* 2018;**516**:210–18.

Wei Yue[1]
Department of Infectious Disease, Yunnan Provincial Key Laboratory of Clinical Virology, The First People's Hospital of Yunnan Province, Kunming, China

Yue Feng[1*], Yuanyuan Jia[1], Yang Liu, Yaxiang Zhang
Faculty of Life Science and Technology, Kunming University of Science and Technology, Kunming, China

Jiawei Geng*
Department of Infectious Disease, Yunnan Provincial Key Laboratory of Clinical Virology, The First People's Hospital of Yunnan Province, Kunming, China

Xueshan Xia*
Faculty of Life Science and Technology, Kunming University of Science and Technology, Kunming, China

*Corresponding authors.
E-mail addresses: fyky2005@163.com (Y. Feng), jia_wei_geng@163.com (J. Geng), oliverxia2000@aliyun.com (X. Xia)

[1] These authors contributed equally in this work.

Accepted 26 November 2019
Available online 29 November 2019

https://doi.org/10.1016/j.jinf.2019.11.019

High risk of hepatitis B virus reactivation among patients treated with direct-acting antivirals and coinfected with HCV and HIV

We recently read the article by Corma-Gómez A. et al. on which the authors described a higher probability of relapses with sofosbuvir/ledipasvir 8 weeks compared with 12 weeks of HCV (hepatitis C virus) among HIV (human immunodeficiency virus)/HCV coinfected patients.[1] In this regard, coinfections of HIV/ HCV also with hepatitis B virus (HBV) is associated with high mortality and comorbidity too. The persistence of HBV DNA within the core cell in the absence of HBsAg and even after clearance of the infection has been described previously in immunosuppressed patients, where HBV screening and prophylaxis is recommended.[2] Interestingly, HBV reactivation has recently emerged during or after HCV treatment with direct-acting antivirals (DAA).[3–5] The US Food and Drug Administration issued a warning about this risk in 2016,[6] until that moment 24 cases were reported, two of which died. Although specific mechanisms of this event are not well known, it has been suggested that HCV core proteins could inhibit HBV replication and HBsAg production as well as production of envelope proteins, being HBcAb the only marker of the presence of HBV.[2] In this context, treatment with DAA would produce a drastic and rapidly blocking of HCV replication providing the opportunity to HBV to emerge and produce an immune reconstitution syndrome.

The interference HBV–HCV has been outlined in 24% of patients with chronic HBV infection (HBsAg-positive serology) and 1.4% of patients with resolved HBV infections (HBsAg-negative and HBcAb-positive) in a recently published systematic review and meta-analysis of patients with HCV–HBV.[7] In most cases, these reports have focused on coinfection HCV–HBV, but there is still a concern about patients triple-infected with HCV, HBV and HIV.

Although most cases reported occur in HBsAg-positive, the main concern affects to patients with a basal serology showing HBcAb-positive, HBsAg-negative and HBsAb-negative. HBsAg-positive was associated with higher rates of HBV reactivations compared with HBsAg-negative and HBcAb-positive patients.[8] There is no clear information about this issue in HBsAg-negative, HBcAb-positive, and, when occurs, it is considered an uncommon event.[9]

Reactivation of HBV is characterized by reappearance or increase in HBV DNA levels, and could also be accompanied by symptoms of hepatitis. The cases reported previously did show difference in the time of presentation of clinical symptoms, they used to start either during or after DAA treatment. It seems that HBV reactivation usually occurs early after DAA initiation treatment (4–8 weeks) while otherwise can occur after treatment completion. In that way, it seems necessary that HBV infection should be monitored early after DAA initiation.

The most recent European Association for the Study of the Liver (EASL) guideline about HBV infection, recommends that patients HBsAg-negative and HBcAb-positive undergoing DAA treatment should be monitored and tested for HBV reactivation only in case of ALT elevation.[10] They also recommend performing HBV DNA levels only in case of ALT increase. At the same time, the American Association for the Study of Liver Diseases (AASLD) and the Infectious Disease Society of America (IDSA) guideline has been recently updated recommendations to monitor HBV DNA levels only in patients HBsAg-positive, but they emphasize that there is not enough data to monitoring DNA among patients HBcAb-positive or HBcAb-positive and HBsAb-positive. They remark that a reactivation should be considered if an unexplained increase in liver enzyme is present. In HIV patients, they provide the same recommendations.[11] In a recent review of the literature, the authors also recommend to perform an HBV DNA only in patients with altered ALT.[9] A meta-analysis recommended not to perform an HBV DNA test in this case due to low rate of incidence and the associated cost which needs to be considered especially in an endemic HBV areas.[7] Few data exist in HIV patients. The fact that many triple-infected patients are receiving antiretroviral therapy including (ART) nucleoside/nucleotide analogous, as tenofovir disoproxil fumarate (TDF) or tenofovir alafenamide (TAF), both active against HBV, suggest that HBV reactivation rate could be underestimated. In a recently published review, Chang et al., recommend to perform an HBV DNA test at baseline in triple-infected patients. If positive, an HBV-active antiretroviral therapy (ART) should be started and HBV DNA needs to be monitored every 4 weeks during treatment and until week 12 after completion of treatment. However, if baseline HBV DNA is negative they match with AASLD/IDSA and EASL recommendations.[12]

One of our patients has a basal serology with HBcAb-IgG-positive, both HBsAg- and HBsAb-negatives, and undetectable HBV DNA levels, prior to treatment with DAAs. Regarding HIV infection, he has an analogues-free regimen. One month after having finished treatment with DAAs, the patient consulted because of abdominal pain, nausea and jaundice. He had a total bilirubin level of 11 mg/dl, AST 1025 IU/l, ALT 642 IU/l and INR 1.30. A HBV viral load of 6,193,455 IU/mL was detected; HBsAg, HBcAb-IgM and HBeAg were positive. There were no reasons to believe that he was re-infected. Treatment with entecavir was initiated; however, the clinical evolution was unfavorable and died as a result of an acute liver failure. The HBV viral load was requested from the stored samples drawn during the treatment of HCV showing that HBV viral load was undetectable at the beginning of treatment and in week 2, but progressively increased to 98 IU/mL in week 8 and up to 82,700 IU/mL in week 4 after treatment completion. During the follow-up of DAA treatment ALT and AST remained normal. This case changed our daily practice, since then all HIV patients and more specifically those not treated with either TDF or TAF and presenting a previous HBcAb-positive, are followed using DNA levels and not only monitoring hepatic enzymes, as recommended by guidelines. We consider that this case may reflect the necessity of change the current guidelines. We recommend to perform a periodic monitoring of HBV reactivation using HBV DNA during and after DAA therapy in HBsAg-negative and HBcAb-positive patients, independently of HBsAb presence, hepatic enzymes and clinical symptoms, particularly in HIV patients who are not receiving active treatment of HBV.

Financial support

The study was not funded.

Declaration of Competing Interest

Authors declare that there is no conflict of interest.

References

1. Corma.Gómez A., Macías J., Merino Muñoz D., Téllez F., Granados R., Morano L.E., et al. Higher relapse rate among HIV/HCV-confected patients receiving sofosbuvir/ledipasvir for 8 vs 12 weeks. *J Infect* 2019;**79**(1):30–5. doi:10.1016/j.jinf.2019.05.005.
2. Wang Q., Klenerman P., Semmo N.. Significance of anti-HBc alone serological status in clinical practice. *Lancet Gastroenterol Hepatol* 2017;**2**(2):123–4.
3. Belperio P.S., Shahoumian T.A., Mole L.A., Backus L.I.. Evaluation of hepatitis B reactivation among 62,920 veterans treated with oral hepatitis C antivirals. *Hepatology* 2017;**66**(1):27–36.
4. Paniagua-García M., López-Hernández I., Fernández-Cuenca F., Ríos-Villegas M.J.. Acute fulminant hepatitis B during hepatitis C virus therapy with direct-acting antivirals in a patient co-infected with HIV. *Enferm Infecc Microbiol Clin* 2017;**35**(10):681–2.
5. Sato K., Kobayashi T., Yamazaki Y., Takakusagi S., Horiguchi N., Kakizaki S., et al. Spontaneous remission of hepatitis B virus reactivation during direct-acting antiviral agent-based therapy for chronic hepatitis C. *Hepatol Res* 2017;**47**(12):1346–53.
6. US Food and Drug Administration. Adverse events reporting system (FAERS): the public's stake in adverse event reporting. https://www.fda.gov/drugs/guidancecomplianceregulatoryinformation/surveillance/adversedrugeffects/ucm179586.htm. Updated April 10, 2016. Accessed May 16, 2018.
7. Mücke M.M., Backus L.I., Mücke V.T., Coppola N., Preda C.M., Yeh M.L., et al. Hepatitis B virus reactivation during direct-acting antiviral therapy for hepatitis C: a systematic review and meta-analysis. *Lancet Gastroenterol Hepatol* 2018 2018 Jan 19. pii: S2468-1253(18)30002-5.
8. Yeh M.-L., Huang C.-F., Hsieh M.-H., Ko Y.M., Chen K.Y., Liu T.W., et al. Reactivation of hepatitis B in patients of chronic hepatitis C with hepatitis B virus infection treated with direct acting antivirals. *J Gastroenterol Hepatol* 2017;**32**(10):1754–62.
9. M.D. Lieber S.R., Fried M.W.. Controversies in hepatitis C therapy: reactivation of hepatitis B virus. *Clin Liver Dis* 2017;**10**:87–92.
10. European Association for the Study of the Liver. EASL 2017 Clinical Practice Guidelines on the management of hepatitis B virus infection. Electronic address: http://www.easl.eu/medias/cpg/management-of-hepatitis-B-virus-infection/English-report.pdf. European Association for the Study of the Liver. Last access: March 3rd. J Hepatol. 2017;67(2):370–398.
11. Monitoring Patients Who Are Starting HCV Treatment, Are on Treatment, or Have Completed Therapy. HCV Guidance: Recommendations for Testing, Managing, and Treating Hepatitis C. Electronic access: https://www.hcvguidelines.org/evaluate/monitoring. 2019. Last access: December 11th. AASLD and IDSA.
12. Chang J.J., Mohtashemi N., Bhattacharya D.. Significance and management of isolated hepatitis B core antibody (Anti-HBc) in HIV and HCV: strategies in the DAA era. *Curr HIV/AIDS Rep* 2018;**15**(2):172–81.

Zaira R. Palacios-Baena, María Paniagua-García, Inmaculada López-Hernández, Felipe Fernández-Cuenca
Department of Infectious Diseases, Microbiology and Preventive Medicine, University Hospital Virgen Macarena/Institute of Biomedicine of Sevilla (IBIS), Avda. Dr. Fedriani, No 3, 41008 Seville, Spain

Mª José Ríos-Villegas
Department of Infectious Diseases, Microbiology and Preventive Medicine, University Hospital Virgen Macarena/Institute of Biomedicine of Sevilla (IBIS), Avda. Dr. Fedriani, No 3, 41008 Seville, Spain
Department of Medicine, University of Seville, Seville, Spain

*Corresponding author.
E-mail addresses: zaira.palacios.baena@hotmail.com, zpalacios@us.es (Z.R. Palacios-Baena)

Accepted 26 November 2019
Available online 5 December 2019

https://doi.org/10.1016/j.jinf.2019.11.018

The heterogeneity of influenza seasonality by subtype and lineage in China

Dear Editor,

Recently, a notable pattern of synchrony of influenza A and B virus, and respiratory syncytial virus incidence peaks globally was reported in this journal.[1] A previous study characterized seasonal pattern of influenza A and B in China and identified three epidemiological regions featured by distinct seasonality.[2] On the basis of laboratory surveillance data from 30 Chinese provinces spanning about 12 years from October 2004 through January 2017, our study further characterized seasonal patterns of circulating influenza A subtypes and influenza B lineages in the three defined epidemiological regions. Our study revealed that pre-2009 A(H1N1) and A(H3N2) displayed wintertime and summertime epidemics in mid-latitude and southernmost Chinese provinces with subtropical climate, wavelet analysis demonstrated the two subtypes displayed twice-annual cycle in some years in mid-latitude Chinese provinces (Fig. 1(a)–(h)). However, the two subtypes peaks in the winter with annual or longer cycle in northern Chinese provinces. Influenza A(H1N1)pdm09 B/Victoria and B/Yamagata virus all displayed epidemics in the winter or winter-spring with annual or longer cycle in all three epidemiological regions.

We developed univariate and multivariate regression models to evaluate the association between climatic factors and the presence or absence of epidemics of each influenza subtype and lineage (positive proportion≥5%) in the southernmost provinces where heating system is not generally used in the winter so temperature and relative humidity in external conditions in winter are close to those in indoor environment where people spend most of the time. We fitted the mixed-effects logistic regression model to control for the repeated measurements in each province of the region cluster. We kept one of temperature and absolute humidity (representative of vapor pressure) with smaller Akaike information criterion in the model to reduce of multi-collinearity due to a high degree of correlation between the two factors.

Our analysis indicated temperature, humidity and rainfall were environmental predictors of influenza subtype/lineage-specific epidemics in the southernmost provinces when a 1-week lag of influenza epidemics behind climate was considered, which was similar to the findings from some ecological studies (Table 1).[3] Our study indicated the U-shaped relationship between absolute humidity (AH) and pre-2009 A(H1N1) or A(H3N2) epidemics in the southernmost provinces, and suggest that high levels of AH in the summer, and low levels of AH in the winter increased the possibility of epidemics of the two subtypes.[3] In our analysis, lower temperature was an environmental driver of A (H1N1)pdm09 and B/Yamagata epidemics in the southernmost provinces while there were bimodal associations between temperature, rainfall and B/Victoria epidemics with highest probability of B/Victoria epidemics at 11.7 °C of daily average temperature and 11.3 mm of daily average rainfall.

Although seasonal changes in human behaviors, such as school attendance or crowding indoors, and seasonal variations in immunity, such as melatonin and vitamin D levels have been proposed to account for the seasonal nature of influenza,[4] our findings suggest that the heterogeneity in influenza subtype/lineage-specific seasonality patterns could be driven by seasonal variations in virus survival, transmission and adaptive immunity by influenza subtype and lineage because of the same behavior modes and background of non-adaptive immunity in the same regions and seasons. We propose a hypothesis: under humid and hot condition the dominant transmission mode(s) for A(H1N1)pdm09, B/Victoria and B/Yamagata might have reduced efficiency, however, there could be effective transmission mode(s) for A(H3N2) and pre-2009 A(H1N1) virus.

Some experimental studies were performed to establishing a causal link between humidity, temperature and influenza virus survival/transmission.[5] Transmission of influenza A (H3N2), A(H1N1)pdm09, B/Victoria and B/Yamagata virus by respiratory droplets or aerosols in the guinea pig model proceeds most readily under cold, dry conditions.[5] Low humidity and temperature increased the stability of influenza virus in aerosols and on surfaces. Furthermore, aerosol transmission of A (H3N2) virus in the guinea pig model was almost completely blocked at 30 °C, but contact transmission of A (H3N2) virus seemed to be efficient at different level of humidity and 30 °C.[5] It remains unclear if high temperature and humidity levels have effect on aerosol and contact transmission of pre-2009 A(H1N1), A(H1N1)pdm09, B/Victoria and B/Yamagata virus among hosts and their stability on surfaces. Of note, an experimental study found the survival durations of A(H3N2) strains on Swiss banknotes were significantly longer than pre-2009 A(H1N1) and B/Victoria virus.[6] Further studies are needed to understand how efficient are these transmission modes for different influenza subtypes or lineages, which is/are dominant mode(s) of transmission among hosts, and which of potential mechanisms is at play under humid and hot condition.

One of our findings was the mutual inverse association between A(H3N2) and A(H1N1)pdm09 epidemics, which provided the evidence on interference between the two influenza A subtypes perhaps possibly due to multiple immune mechanisms.[7] However, our study showed B/Yamagata epidemics were positively correlated with A(H3N2) epidemics, suggesting B/Yamagata epidemics across over 12 study years that were weak could get well along with simultaneous weak H3N2 epidemics.

Understanding of influenza seasonality is important to define optimal timing of influenza vaccination campaigns. Our study indicated that A(H3N2) virus brought about twice-annual epidemics in some years in mid-latitude Chinese provinces and more frequent summertime epidemics in southernmost Chinese provinces, which questions if a single annual influenza vaccination campaign starting in October can offer optimal protection against summertime epidemics of A (H3N2) virus in mid-latitude and southernmost Chinese provinces. In recent years, It has been reported that mismatches of A(H3N2) virus between the influenza vaccine strains and circulating strains were identified frequently,[8] and vaccine effectiveness of A(H3N2) virus declined within 4–6 months post-vaccination.[9]

In conclusion, we identified the heterogeneity of seasonality pattern of pre-2009 A(H1N1) or A(H3N2) virus in three epidemiological regions of China, and different environment predictors for influenza subtypes and lineages in the southernmost provinces. Further work should focus on understanding difference in virus survival, transmission by influenza subtype and lineage under humid and hot conditions.

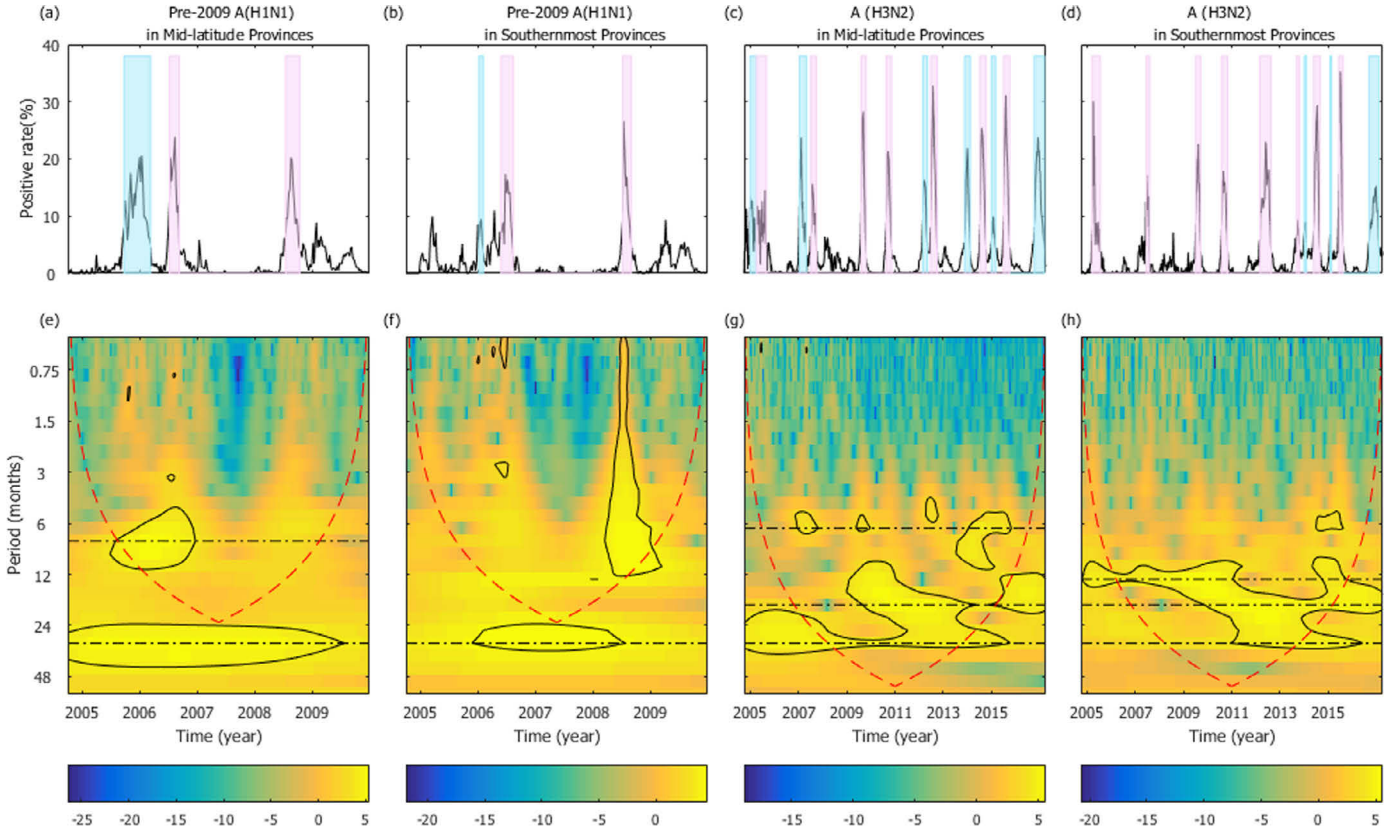

Fig. 1. Wavelet analysis for pre-2009 influenza A (H1N1) and A (H3N2) activity in mid-latitude and southernmost Chinese provinces. (a)–(d) The time series of the weekly percent of specimens positive for pre-2009 influenza A (H1N1) and A (H3N2) virus in mid-latitude and southernmost Chinese provinces respectively. The skyblue bars show defined epidemics of pre-2009 influenza A (H1N1) and A (H3N2) virus peaking in the winter. The pink bars show defined epidemics of pre-2009 influenza A (H1N1) and A (H3N2) virus peaking in the summer. (e)–(h) Wavelet power spectrum of pre-2009 influenza A (H1N1) and A (H3N2) virus activity in mid-latitude and southernmost Chinese provinces respectively. The black contour lines show the regions of power significant at the 5% level. The cones of influence (black curves) indicate the region without edge effects. The power values are coded from dark blue for low power to light yellow for high power, as shown in the bottom panel.

Table 1
Environmental predictors of influenza subtype/lineage-specific epidemics in southernmost Chinese provinces.

	Pre-2009 A (H1N1)coefficients (SE)	A(H1N1)pdm09 coefficients (SE)	A (H3N2) coefficients (SE)	B/Victoria Coefficients (SE)	B/Yamagata coefficients (SE)
Vapor pressure	−0.30 (0.08)		−0.24 (0.05)		
(Vapor pressure)^2	8.35e−3 (1.85e−3)		8.01e−3 (1.12e−3)		
Daily average temperature				0.12 (0.03)	−0.07 (0.02)
(Daily average temperature)^2		−4.37e−3 (5.59e−4)		−5.11e−3 (1.60e−3)	
Relative humidity	0.06	0.05 (0.01)			
(Relative humidity)^2					
Precipitation			0.06 (0.02)	0.14(0.06)	
(Precipitation)^2			−2.15e−3 (8.63e−4)	−6.19e−3 (1.44e−3)	
Pre-2009 A (H1N1) or A (H1N1)pdm09 epidemics			−0.54 (0.15)		
A (H3N2) epidemics		−1.05 (0.29)			0.69 (0.16)

a. Environmental predictors of influenza subtype-specific peaks lagged 1 week behind climate in southernmost Chinese provinces were shown.
b. Vapor pressure represents absolute humidity.

Declaration of Competing Interest

BJC has received research funding from MedImmune Inc. and Sanofi Pasteur, and consults for Crucell NV. The authors report no other potential competing interests.

Ethics approval and consent to participate

As this study included data from the National Influenza Surveillance System, ethics approval was not required.

Consent for publication

Not applicable.

Research data for this article

The datasets at national level analyzed during the current study are available in the World Health Organization Flunet. The datasets with more specific information analyzed during the current study are available in Chinese National Influenza Surveillance Informatio System, but they are not open-access datasets. These Influenza

surveillance data can be available from Chinese National Influenza Center on reasonable request.

Funding

This study was supported by the National Mega-projects for Infectious Diseases (grant number 2018ZX10201002-008-001), National Natural Science Foundation of China (grant number 81302476) and Emergency Prevention and Control Project of Ministry of Science and Technology (grant number 10600100000015001206). The funding bodies had no role in study design, data collection and analysis, preparation of the manuscript, or the decision to publish.

Acknowledgments

We thank Chinese National Influenza Surveillance Network for contribution in influenza epidemiological and laboratory surveillance.

References

1. Lam T.T., Tang J.W., Lai F.Y., Zaraket H., Dbaibo G., Bialasiewicz S., et al. Comparative global epidemiology of inßuenza, respiratory syncytial and parainßuenza viruses, 2010–2015. *J Infection* 2019;**79**(4):373–82.
2. Yu H., Alonso W.J., Feng L., Tan Y., Shu Y., Yang W., et al. Characterization of regional influenza seasonality patterns in China and implications for vaccination strategies: spatio-temporal modeling of surveillance data. *PLoS Med* 2013;**10**(11):e1001552.
3. Tamerius J.D., Shaman J., Alonso W.J., Bloom-Feshbach K., Uejio C.K., Comrie A., et al. Environmental predictors of seasonal influenza epidemics across temperate and tropical climates. *PLoS Pathog* 2013;**9**(3):e1003194.
4. Tamerius J., Nelson M.I., Zhou S.Z., Viboud C., Miller M.A., Alonso W.J.. Global influenza seasonality: reconciling patterns across temperate and tropical regions. *Environ Health Perspect* 2011;**119**(4):439–45.
5. Lowen A.C., Steel J.. Roles of humidity and temperature in shaping influenza seasonality. *J Virol* 2014;**88**(14):7692–5.
6. Thomas Y., Vogel G., Wunderli W., Suter P., Witschi M., Koch D., et al. Survival of influenza virus on banknotes. *Appl Environ Microbiol* 2008;**74**(10):3002–7.
7. DaPalma T D.B., Trager N.M., Kasman L.M.. A systematic approach to virus-virus interactions. *Virus Res* 2010;**149**:1–9.
8. Tricco A.C, Soobiah C., Hallett D., Meier G., Chen M.H., Tashkandi M., Bauch C.T., Loeb M.. Comparing influenza vaccine efficacy against mismatched and matched strains a systematic review and meta-analysis. *BMC Med* 2013;**11**:153.
9. Kissling E., Nunes B., Robertson C., Valenciano M., Reuss A., Larrauri A., et al. I-MOVE multicentre case-control study 2010/11 to 2014/15: Is there within-season waning of influenza type/subtype vaccine effectiveness with increasing time since vaccination? *Euro Surveill* 2016;**21**(16).

Cuiling Xu
Chinese National Influenza Center, National Institute for Viral Disease Control and Prevention, Collaboration Innovation Center for Diagnosis and Treatment of Infectious Diseases, Chinese Center for Disease Control and Prevention, Key Laboratory for Medical Virology, National Health and Family Planning Commission, Beijing, P.R. China

Benjamin J. Cowling
WHO Collaborating Centre for Infectious Disease Epidemiology and Control, Li Ka Shing Faculty of Medicine, The University of Hong Kong, Hong Kong Special Administrative Region, China

Tao Chen, Lijie Wang, Ye Zhang
Chinese National Influenza Center, National Institute for Viral Disease Control and Prevention, Collaboration Innovation Center for Diagnosis and Treatment of Infectious Diseases, Chinese Center for Disease Control and Prevention, Key Laboratory for Medical Virology, National Health and Family Planning Commission, Beijing, P.R. China

Dawei Huang
Institute of Artificial Intelligence and Robotics, Xi'an Jiaotong University

Lei Yang, Jing Yang, Weijuan Huang, Dayan Wang**
Chinese National Influenza Center, National Institute for Viral Disease Control and Prevention, Collaboration Innovation Center for Diagnosis and Treatment of Infectious Diseases, Chinese Center for Disease Control and Prevention, Key Laboratory for Medical Virology, National Health and Family Planning Commission, Beijing, P.R. China

Yuelong Shu*
Chinese National Influenza Center, National Institute for Viral Disease Control and Prevention, Collaboration Innovation Center for Diagnosis and Treatment of Infectious Diseases, Chinese Center for Disease Control and Prevention, Key Laboratory for Medical Virology, National Health and Family Planning Commission, Beijing, P.R. China
School of Public Health (Shenzhen), Sun Yat-sen University, Guangdong, P.R. China

*Corresponding author: Yuelong Shu, Public Health School (Shenzhen), Sun Yat-sen University. No.135 Xingangxi Road, Guangzhou, 510275, P. R. China.
**Dayan Wang, National Institute for Viral Disease Control and Prevention, Chinese Center for Disease Control and Prevention. No.155 Changbai Road, Changping District, Beijing, 102206, P. R. China.
E-mail addresses: dayanwang@cnic.org.cn (D. Wang), yshu@cnic.org.cn (Y. Shu)

Accepted 26 November 2019
Available online 30 November 2019

https://doi.org/10.1016/j.jinf.2019.11.017

Nonindigenous East/Central/South African genotype of chikungunya virus identified in febrile returning travellers in Yunnan, China

Dear Editor,

Recent correspondence in this Journal has highlighted the current threat posed by recently-emerging imported chikungunya virus (CHIKV) in febrile returning travellers.[1] Chikungunya fever is infection caused by the CHIKV and is characterized by fever, arthralgia, myalgia, headache, and rash. CHIKV belongs to the genus *Alphavirus* within the *Togaviridae* family and is transmitted to humans by the bite of infected mosquitoes—*Ae. aegypti* and *Ae. albopictus*.[2] Since the first report of CHIKV infection in humans in Tanzania, intermittent outbreaks have been documented in Africa, South America, Southern and Southeastern Asia, and the Indian Ocean Islands; thus, its outbreak has become a global public health problem.[3]

To date, three evolutionary distinct CHIKV genotypes, namely West African (WA), East/Central/South African (ECSA), and Asian have been identified, based on phylogenetic analyses.[4] A novel lineage of CHIKV—the Indian Ocean lineage (IOL)—has also been reported, which descended from the ECSA genotype during an outbreak on the island of La Reunion between 2005 and 2006.[5] Recently, it has been reported that IOL of CHIKV has spread to Malaysia, Singapore, Thailand, and Indonesia.[6]

In China, the first case of imported CHIKV infection was found in Yunnan in 1987. Subsequently, several sporadic cases of non-indigenous CHIKV infection have been described. In 2010, the first outbreak of CHIKV fever with 129 cases was documented in Guangdong.[7] Recently, another outbreak of Chikungunya fever was

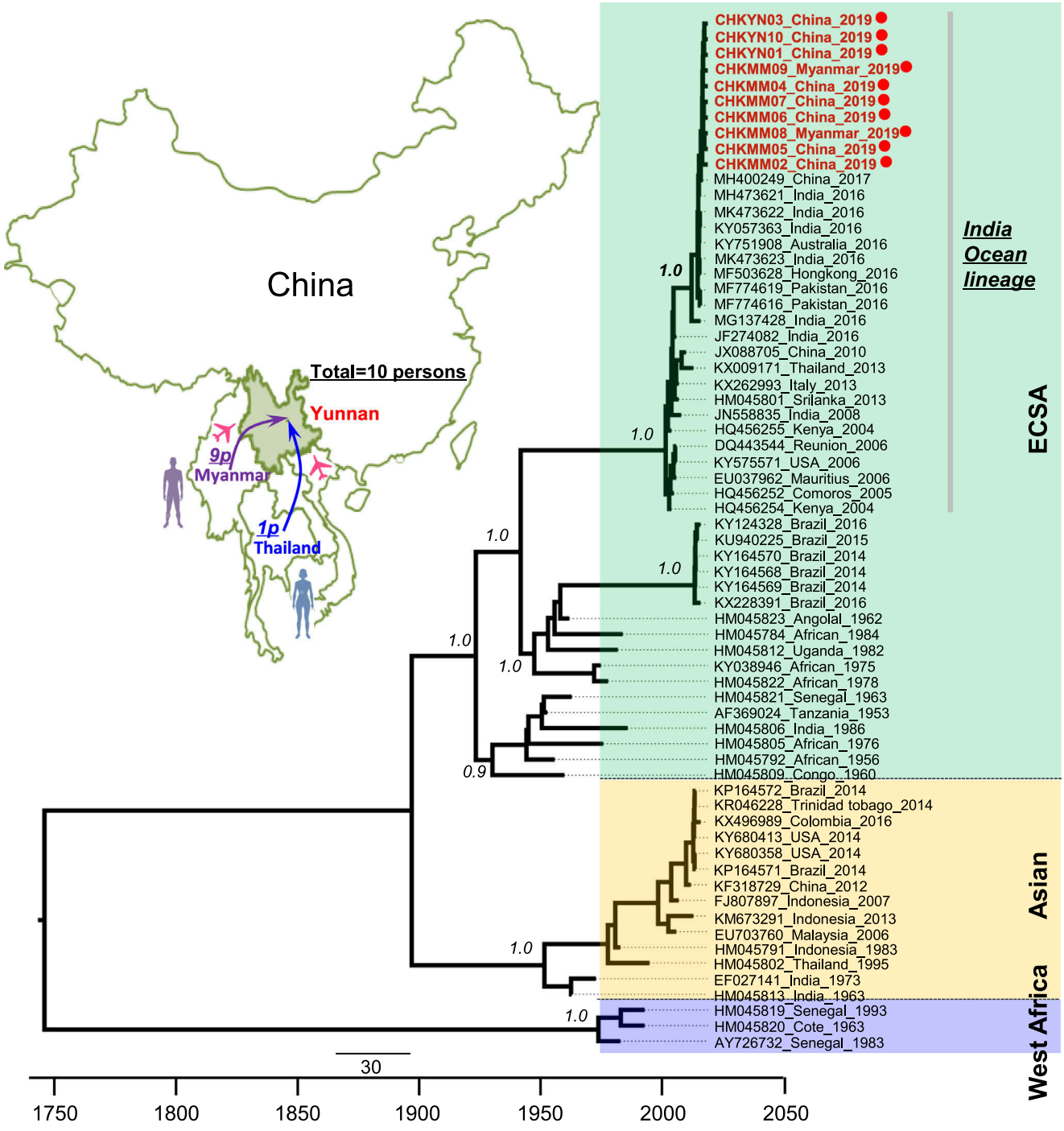

Fig. 1. Maps of the study region, phylogenetic analysis of maximum clade credibility (MCC) tree based on the complete genome sequences of the ten CHIKV strains isolated from serum samples. (A) Ten cases of imported CHIKV infection in travelers returning to Yunnan from Southeastern Asia in 2019, of which nine CHIKV infections had traveled back from Myanmar and one from Thailand. (B) Temporal maximum clade credibility tree of the complete CHIKV genomic sequence obtained from positive serum samples was constructed based on an uncorrelated exponential distributed relaxed-clock model for our sample. The genotypes of CHIKV were divided into West African, ECSA, and Asian. Virus lineages are shown at right. The numbers on the branches represent the posterior probability values. CHIKV, chikungunya virus; ECSA, East/Central/South African.

reported in Zhejiang in 2017.[8] In this study, we identified ten cases of imported CHIKV infection in travelers returning to Yunnan from Southeastern Asia in 2019.

Out of the ten patients with imported CHIKV infection examined in this study, nine patients had traveled back from Myanmar and one patient had travelled back from Thailand (Fig. 1(A)). All the patients displayed different degrees of symptoms, such as fever, cough, muscle pain, and rash. The details of all the symptoms are shown in Table 1. CHIKV infection was diagnosed using specific real-time reverse transcription-PCR. Serum specimens were collected from the ten patients that tested positive for CHIKV by real-time PCR analysis, in Yunnan between May 7, 2019 and August 1, 2019. The current study was approved by the Medical Ethics Committee of Kunming University of Science and Technology. Written informed consent was obtained from all the participants.

Table 1
Epidemiological information on ten febrile returning travelers infected with CHIKV in this study.

ID	Traveling abroad history	Nationality	Sample	Sampling date	Patient sex	Patient age (years)	Clinical symptoms
CHKYN01	Thailand	China	Serum	05/07/2019	F	25	Fever (38.9 °C), muscle pain, rash
CHKYN02	Myanmar	China	Serum	05/09/2019	M	49	Fever (37.9 °C), cough
CHKYN03	Myanmar	China	Serum	06/26/2019	M	43	Fever (38.9 °C), cough
CHKYN04	Myanmar	China	Serum	07/02/2019	M	22	Fever (39.3 °C), headache, chills
CHKYN05	Myanmar	China	Serum	07/25/2019	M	24	Fever (39.1 °C), cough
CHKYN06	Myanmar	China	Serum	07/26/2019	M	43	Fever (39.2 °C), headache, muscle pain
CHKYN07	Myanmar	China	Serum	07/29/2019	M	24	Fever (39.0 °C), chills, headache, vomit, blocked nose
CHKYN08	Myanmar	Myanmar	Serum	07/31/2019	M	35	Fever (37.6 °C), cough
CHKYN09	Myanmar	Myanmar	Serum	07/31/2019	M	34	Fever (37.8 °C), cough
CHKYN10	Myanmar	China	Serum	08/01/2019	M	43	Fever (37.8 °C), cough

In this study, nine complete genome sequences isolated from serum samples were successfully amplified and sequenced with 12 overlapping fragments, and then the sequence obtained was deposited in GenBank under accession no. MN402883-MN402892. Compared with the nucleotide sequences of the available from the NCBI database, the nine strains shared the highest 99.61–99.74% nucleotide identity with the East/Central/South African lineage strain Thail 2019 reported previously in Thailand, 2019. Further, Bayesian maximum-clade-credibility tree for full-length nucleotide sequences were constructed using the BEAST package v.1.7.3. Phylogenetic analyses revealed that the ten CHIKV strains clustered into the homogeneous Indian Ocean clade of the ECSA genotype (Fig. 1(B)).

Notably, the ten CHIKV strains isolated from serum samples possessed the mutation K211E in the E1 gene and V264A in the E2 gene; these mutations are associated with significant increase in viral infectivity in *Ae. aegypti*.[9] The strains also possessed G60D and I211T substitutions in the E2 gene; these mutations contribute to increased CHIKV fitness in *Ae. albopictus*.[9] However, the A226V mutation in the E1 gene that is related to significant increase in viral infectivity in *Ae. albopictus* was not observed in any of the strains.[10]

In summary, we characterized ten cases of human infection caused by imported ECSA genotype CHIKV in Yunnan, China and successfully isolated nine infectious CHIKVs from the CHIKV-positive serum samples. The mutations associated with significant increase in viral infectivity for *Ae. aegypti* or *Ae. albopictus* were also observed in these strains. Geographically, the Yunnan province is in southeastern China and shares its border with Southeast Asian countries (Laos, Vietnam, and Myanmar) that are most affected by CHIKV. With the increase of tourism and trade with Southeast Asian countries, cases of imported CHIKV infection are constantly increasing and may have the potential for re-emergence and autochthonous transmission to Yunnan. The present study highlights the urgent need for continuous molecular screening and epidemic surveillance for CHIKV and its vectors to prevent future outbreaks of CHIKV infection among the human population of Yunnan.

Financial support

This work was supported by the National Natural Science Foundation of China (NSFC) (U1702282), the Reserve Talents Project for Young and Middle-Aged Academic and Technical Leaders of Yunnan Province (2019HB012), and Youth Talent Program of Yunnan "Ten-thousand Talents Program" (YNWR-QNBJ-2018-054).

Declaration of Competing Interest

The authors declare no competing financial interests.

Acknowledgments

We thank the members of the Yunnan international travel healthcare center and Kunming Changshui airport customs for the data and sample collection.

References

1. Jerome H., Taylor C., Sreenu V.B., Klymenko T., Filipe A.D.S., Jackson C., et al. Metagenomic next-generation sequencing aids the diagnosis of viral infections in febrile returning travellers. *J Infect* 2019;**79**(4):383–8.
2. Frickmann H., Herchenröder O.. Chikungunya virus infections in military deployments in tropical settings-a narrative minireview. *Viruses* 2019;**11**(6):E550.
3. Burt F.J., Chen W., Miner J.J., Lenschow D.J., Merits A., Schnettler E., et al. Chikungunya virus: an update on the biology and pathogenesis of this emerging pathogen. *Lancet Infect Dis* 2017;**17**(4):e107–17.
4. Rahman M., Yamagishi J., Rahim R., Hasan A., Sobhan A. East/Central/South African genotype in a Chikungunya outbreak, Dhaka, Bangladesh, 2017. *Emerg Infect Dis* 2019;**25**(2):370–2.
5. Teo T.H., Her Z., Tan J.J., Lum F.M., Lee W.W., Chan Y.H., et al. Caribbean and la réunion chikungunya virus isolates differ in their capacity to induce proinflammatory Th1 and NK cell responses and acute joint pathology. *J Virol* 2015;**89**(15):7955–69.
6. Pyke A.T., Moore P.R., McMahon J. New insights into chikungunya virus emergence and spread from southeast Asia. *Emerg Microbes Infect* 2018;**7**(1):26.
7. Xia H., Wang Y., Atoni E., Zhang B., Yuan Z. Mosquito-associated viruses in China. *Virol Sin* 2018;**33**(1):5–20.
8. Pan J., Fang C., Yan J., Yan H., Zhan B., Sun Y., et al. Chikungunya fever outbreak, Zhejiang province, China, 2017. *Emerg Infect Dis* 2019;**25**(8):1589–91.
9. Fischer C., de Lamballerie X., Drexler J.F. Enhanced molecular surveillance of Chikungunya virus. *mSphere* 2019;**4**(4) e00295-19.
10. Tsetsarkin K.A., Chen R., Leal G., Forrester N., Higgs S., Huang J., et al. Chikungunya virus emergence is constrained in Asia by lineage-specific adaptive landscapes. *Proc Natl Acad Sci USA* 2011;**108**(19):7872–7.

Yue Feng[1*], Hui Xiao[1]
Faculty of Life Science and Technology, Kunming University of Science and Technology, No. 727 Jing Ming Road, Chenggong District, Kunming, China

Xiaofei Li[1]
Department of Clinical Laboratory, The Third People's Hospital of Kunming City, Kunming, China

Yunlan Lu, Jie Li
Yunnan international travel healthcare center, Kunming, China

Mengyuan Zheng
Faculty of Life Science and Technology, Kunming University of Science and Technology, No. 727 Jing Ming Road, Chenggong District, Kunming, China

Dongbiao Lv, Wei Yuan, Ziyang Zhang, Yan Zhou
Kunming Changshui airport customs, Kunming, China

Yuebo Liang, Weihong Qin[*]
Yunnan international travel healthcare center, Kunming, China

Xueshan Xia*
Faculty of Life Science and Technology, Kunming University of Science and Technology, No. 727 Jing Ming Road, Chenggong District, Kunming, China

*Corresponding authors.
E-mail addresses: fyky2005@kust.edu.cn (Y. Feng), qinwh19@sina.com (W. Qin), oliverxia2000@aliyun.com (X. Xia)

[1] These first authors contributed equally in this work.
Accepted 23 December 2019
Available online 28 December 2019

https://doi.org/10.1016/j.jinf.2019.12.014